for technical assistance, and Kieko Segawa for secretarial work. This study was supported by a grant from the Japan Cardiovascular Research Foundation; by Grants-in-Aid for Human Genome, Tissue Engineering and Food Biotechnology (H13-Genome-011) and for Comprehensive Research on Aging and Health [H13-21 seiki (seikatsu)-23], both Health and Labour Sciences Research Grants from the Ministry of Health, Labor, and Welfare; by the Takeda Science Foundation; and by a Grant-in-Aid for Scientific Research (No. 17390229) from the Ministry of Education, Science, and Culture of Japan.

## References

[1] M.B. Kastan, D.S. Lim, The many substrates and functions of ATM, Nat. Rev. Mol. Cell Biol. 1 (2000) 179–186.
[2] C.J. Bakkenist, M.B. Kastan, DNA damage activates ATM through intermolecular autophosphorylation and dimer dissociation, Nature 421 (2003) 499–506.
[3] Y. Shiloh, ATM and related protein kinases: safeguarding genome integrity, Nat. Rev. Cancer 3 (2003) 155–168.
[4] A.J. Morrison, J.A. Kim, M.D. Person, J. Highland, J. Xiao, T.S. Wehr, S. Hensley, Y. Bao, J. Shen, S.R. Collins, J.S. Weissman, J. Delrow, N.J. Krogan, J.E. Haber, X. Shen, Mec1/Tel1 phosphorylation of the INO80 chromatin remodeling complex influences DNA damage checkpoint responses, Cell 130 (2007) 499–511.
[5] Z.H. Wu, Y. Shi, R.S. Tibbetts, S. Miyamoto, Molecular linkage between the kinase ATM and NF-kappaB signaling in response to genotoxic stimuli, Science 311 (2006) 1141–1146.
[6] Y. Shi, S.L. Venkataraman, G.E. Dodson, A.M. Mabb, S. LeBlanc, R.S. Tibbetts, Direct regulation of CREB transcriptional activity by ATM in response to genotoxic stress, Proc. Natl. Acad. Sci. USA 101 (2004) 5898–5903.
[7] M.A. Grenier, S.E. Lipshultz, Epidemiology of anthracycline cardiotoxicity in children and adults, Semin. Oncol. 25 (1998) 72–85.
[8] X. Liu, C.C. Chua, J. Gao, Z. Chen, C.L. Landy, R. Hamdy, B.H. Chua, Pifithrin-alpha protects against doxorubicin-induced apoptosis and acute cardiotoxicity in mice, Am. J. Physiol. Heart Circ. Physiol. 286 (2004) H933–H939.
[9] S.M. DeAtley, M.Y. Aksenov, M.V. Aksenova, B. Harris, R. Hadley, P. Cole Harper, J.M. Carney, D.A. Butterfield, Antioxidants protect against reactive oxygen species associated with adriamycin-treated cardiomyocytes, Cancer Lett. 136 (1999) 41–46.
[10] N. Sarvazyan, Visualization of doxorubicin-induced oxidative stress in isolated cardiac myocytes, Am. J. Physiol. 271 (1996) H2079–H2085.
[11] E.U. Kurz, P. Douglas, S.P. Lees-Miller, Doxorubicin activates ATM-dependent phosphorylation of multiple downstream targets in part through the generation of reactive oxygen species, J. Biol. Chem. 279 (2004) 53272–53281.
[12] C.E. Canman, D.S. Lim, K.A. Cimprich, Y. Taya, K. Tamai, K. Sakaguchi, E. Appella, M.B. Kastan, J.D. Siliciano, Activation of the ATM kinase by ionizing radiation and phosphorylation of p53, Science 281 (1998) 1677–1679.
[13] S. Banin, L. Moyal, S. Shieh, Y. Taya, C.W. Anderson, L. Chessa, N.I. Smorodinsky, C. Prives, Y. Reiss, Y. Shiloh, Y. Ziv, Enhanced phosphorylation of p53 by ATM in response to DNA damage, Science 281 (1998) 1674–1677.
[14] T. Hunter, B.M. Sefton, Transforming gene product of Rous sarcoma virus phosphorylates tyrosine, Proc. Natl. Acad. Sci. USA 77 (1980) 1311–1315.
[15] A.R. Krainer, A. Mayeda, D. Kozak, G. Binns, Functional expression of cloned human splicing factor SF2: homology to RNA-binding proteins, U1 70K, and Drosophila splicing regulators, Cell 66 (1991) 383–394.
[16] S.T. Kim, D.S. Lim, C.E. Canman, M.B. Kastan, Substrate specificities and identification of putative substrates of ATM kinase family members, J. Biol. Chem. 274 (1999) 37538–37543.
[17] Y. Asano, S. Takashima, M. Asakura, Y. Shintani, Y. Liao, T. Minamino, H. Asanuma, S. Sanada, J. Kim, A. Ogai, T. Fukushima, Y. Oikawa, Y. Okazaki, Y. Kaneda, M. Sato, J. Miyazaki, S. Kitamura, H. Tomoike, M. Kitakaze, M. Hori, Lamr1 functional retroposon causes right ventricular dysplasia in mice, Nat. Genet. 36 (2004) 123–130.
[18] O. Seguchi, S. Takashima, S. Yamazaki, M. Asakura, Y. Asano, Y. Shintani, M. Wakeno, T. Minamino, H. Kondo, H. Furukawa, K. Nakamaru, A. Naito, T. Takahashi, T. Ohtsuka, K. Kawakami, T. Isomura, S. Kitamura, H. Tomoike, N. Mochizuki, M. Kitakaze, A cardiac myosin light chain kinase regulates sarcomere assembly in the vertebrate heart, J. Clin. Invest. 117 (2007) 2812–2824.
[19] H. Yamamoto, S. Takashima, Y. Shintani, S. Yamazaki, O. Seguchi, A. Nakano, S. Higo, H. Kato, Y. Liao, Y. Asano, T. Minamino, Y. Matsumura, H. Takeda, M. Kitakaze, Identification of a novel substrate for TNFalpha-induced kinase NUAK2, Biochem. Biophys. Res. Commun. 365 (2007) 541–547.
[20] B. Ghebrehiwet, B.L. Lim, R. Kumar, X. Feng, E.I. Peerschke, gC1q-R/p33, a member of a new class of multifunctional and multicompartmental cellular proteins, is involved in inflammation and infection, Immunol. Rev. 180 (2001) 65–77.
[21] S.K. Petersen-Mahrt, C. Estmer, C. Ohrmalm, D.A. Matthews, W.C. Russell, G. Akusjarvi, The splicing factor-associated protein, p32, regulates RNA splicing by inhibiting ASF/SF2 RNA binding and phosphorylation, EMBO J. 18 (1999) 1014–1024.
[22] X. Xu, D. Yang, J.H. Ding, W. Wang, P.H. Chu, N.D. Dalton, H.Y. Wang, J.R. Bermingham Jr., Z. Ye, F. Liu, M.G. Rosenfeld, J.L. Manley, J. Ross Jr., J. Chen, R.P. Xiao, H. Cheng, X.D. Fu, ASF/SF2-regulated CaMKIIdelta alternative splicing temporally reprograms excitation-contraction coupling in cardiac muscle, Cell 120 (2005) 59–72.

*Original Article*

# Atorvastatin Slows the Progression of Cardiac Remodeling in Mice with Pressure Overload and Inhibits Epidermal Growth Factor Receptor Activation

Yulin LIAO[1], Hui ZHAO[2], Akiko OGAI[1], Hisakazu KATO[2], Masanori ASAKURA[1], Jiyoong KIM[1], Hiroshi ASANUMA[1], Tetsuo MINAMINO[2], Seiji TAKASHIMA[2], and Masafumi KITAKAZE[1]

**The aim of this study was to investigate whether atorvastatin inhibits epidermal growth factor receptor (EGFR) activation in cardiomyocytes *in vitro* and slows the progression of cardiac remodeling induced by pressure overload in mice. Either atorvastatin (5 mg/kg/day) or vehicle was orally administered to male C57BL/6J mice with transverse aortic constriction (TAC). Physiological parameters were obtained by echocardiography or left ventricular (LV) catheterization, and morphological and molecular parameters of the heart were also examined. Furthermore, cultured neonatal rat cardiomyocytes were studied to clarify the underlying mechanisms. Four weeks after TAC, atorvastatin reduced the heart/body weight and lung/body weight ratios (8.69±0.38 to 6.45±0.31 mg/g ($p<0.001$) and 10.89±0.68 to 6.61±0.39 mg/g ($p<0.01$) in TAC mice with and without atorvastatin, respectively). Decrease of LV end-diastolic pressure and the time constant of relaxation, increased fractional shortening, downregulation of a disintegrin and metalloproteinase (ADAM)12, ADAM17 and heparin-binding epidermal growth factor genes, and reduction of the activity of EGFR and extracellular signal-regulated kinase (ERK) were observed in the atorvastatin group. Phenylephrine-induced protein synthesis, phosphorylation of EGFR, and activation of ERK in neonatal rat cardiomyocytes were all inhibited by atorvastatin. These findings indicated that atorvastatin ameliorates cardiac remodeling in mice with pressure overload, and its actions are associated with inhibition of the EGFR signaling pathway. (*Hypertens Res* 2008; 31: 335–344)**

***Key Words*: statins, epidermal growth factor receptor, heart failure, hypertrophy, extracellular signal-regulated kinase**

## Introduction

Although substantial evidence obtained by various clinical trials has demonstrated the efficacy of β-blockers, angiotensin-converting enzyme inhibitors, angiotensin receptor blockers, aldosterone antagonists, and vasodilators for treatment of chronic heart failure (CHF) (*1*), the mortality and morbidity of this serious condition remain high. Therefore, investigation of novel treatments to improve the prognosis of

From the [1]Cardiovascular Division of Medicine, National Cardiovascular Center, Suita, Japan; and [2]Department of Cardiovascular Medicine, Osaka University Graduate School of Medicine, Suita, Japan.

This work was supported by Grants (H13-Genome-011 and H13-21seiki (seikatsu)-23) from the Japanese Ministry of Health, Labour and Welfare. One of the authors (Y.L.) was supported by a grant from the Japan Society for the Promotion of Science (P05228).

Address for Reprints: Masafumi Kitakaze, M.D., Ph.D., Cardiovascular Division of Medicine, National Cardiovascular Center, 5–7–1 Fujishirodai, Suita 565–8565, Japan. E-mail: kitakaze@zf6.so-net.ne.jp

Received April 5, 2007; Accepted in revised form September 2, 2007.

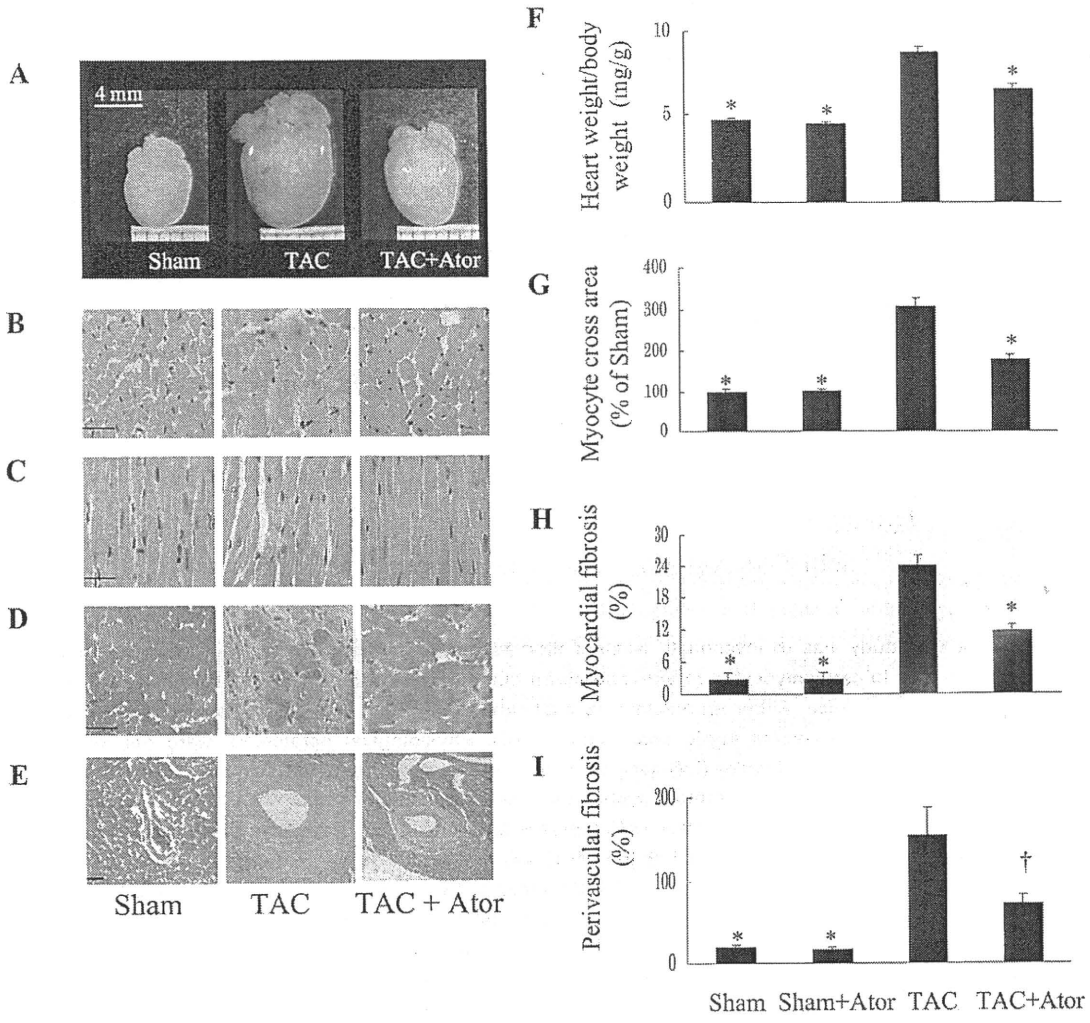


**Fig. 1.** *Effect of atorvastatin (Ator) on cardiac hypertrophy and fibrosis in mice with pressure overload. A: Representative pictures of the whole heart. B: Cardiomyocyte cross-sectional surface area (hematoxylin and eosin stain [H&E stain]). C: Long-axis view of cardiomyocytes (H&E stain). Myocardial fibrosis (D) and perivascular fibrosis (E) are revealed by Azan staining. The heart weight/body weight ratio (HW/BW, ANOVA $p<0.0001$) (F) and cardiomyocyte cross-sectional surface area (ANOVA $p<0.0001$) (G) were significantly reduced in atorvastatin-treated mice. Myocardial fibrosis (ANOVA $p<0.0001$) (H) and perivascular fibrosis (ANOVA $p<0.003$) (I) were also inhibited by atorvastatin. *$p<0.01$, †$p<0.05$ vs. TAC by post-hoc test. In F, the number of mice is 12, 5, 12 and 11 for the sham, sham+Ator, TAC, and TAC+Ator groups, respectively. In G–I, 3–5 hearts from each group were used to obtain data. Bar: 20 μm.*

CHF is an area of intense activity. Recent clinical studies performed by us as well as others have shown that hydroxymethylglutaryl-CoA (HMG-CoA) reductase inhibitors (statins) improve cardiac remodeling and survival in patients with either ischemic or non-ischemic CHF (2–5), suggesting that statin therapy may be a potential new approach for CHF. Randomized double-blind placebo-controlled trials that are still ongoing (6, 7) may eventually provide firm evidence about this issue. In the meantime, well-designed experimental studies will also be helpful to clarify whether statins are beneficial for both systolic and diastolic heart failure, as well as to explore the underlying mechanisms.

Theoretically, several of the many actions of statins may contribute to the improvement of cardiac remodeling. Our previous study demonstrated that myocardial hypertrophy can be induced *via* activation of matrix metalloproteinases (MMPs), which is followed by the subsequent release of heparin binding–epidermal growth factor (HB-EGF) and phosphorylation of the epidermal growth factor receptor (EGFR), and we have shown that an MMP inhibitor can ameliorate

**Table 1. Echocardiographic Findings at 4 Weeks after TAC or Sham Operation**

| Parameters | Sham ($n$=10) | Sham+Ator ($n$=5) | TAC ($n$=11) | TAC+Ator ($n$=11) | ANOVA $p$ value |
|---|---|---|---|---|---|
| LVEDd (mm) | 2.85±0.05* | 2.89±0.08* | 3.22±0.07 | 2.89±0.05* | 0.004 |
| LVPWd (mm) | 0.65±0.01*,† | 0.61±0.02*,† | 0.92±0.02 | 0.74±0.02* | <0.0001 |
| LVESd (mm) | 1.20±0.06* | 1.39±0.12* | 2.10±0.1 | 1.15±0.09* | <0.0001 |
| LVFS (%) | 58±2* | 52±3* | 35±2 | 60±3* | <0.0001 |
| LVEF (%) | 89±1* | 89±3* | 65±3 | 89±2* | <0.0001 |
| HR (bpm) | 543±11 | 540±10 | 490±27 | 527±28 | 0.492 |

TAC, transverse aortic constriction; Ator, atorvastatin; LVEDd, left ventricular end-diastolic dimension; LVPWd, left ventricular diastolic posterior wall thickness; LVESd, left ventricular end-systolic dimension; LVFS, left ventricular fractional shortening; LVEF, left ventricular ejection fraction; HR (bpm), heart rate (beats per minute). *$p$<0.01, †$p$<0.05 compared with TAC, ‡$p$<0.01 *vs.* TAC+Ator. Data are mean±SEM.

cardiac hypertrophy and improve heart failure (*8*). However, it remains unknown whether or not statins inhibit this signal pathway.

Atorvastatin is the most frequently prescribed statin worldwide, but few studies have been performed to clarify its influence on the progression of non-ischemic CHF and the possible cellular mechanisms involved. Accordingly, we investigated whether atorvastatin had a beneficial effect on the morphology and function of the left ventricle in mice with pressure overload, and we also investigated whether inhibition of EGFR activation had a role in the beneficial effects of statin therapy. We found that atorvastatin slowed the progression of cardiac remodeling and inhibited the activation of EGFR and extracellular signal–regulated kinase (ERK).

## Methods

### Transverse Aortic Constriction Model and Experimental Protocol

All procedures were performed in accordance with our institutional guidelines for animal research, which conform to the "Guide for the Care and Use of Laboratory Animals" published by the US National Institutes of Health (NIH Publication No. 85-23, revised 1996). Male C57BL/6J mice (7–8 weeks old and weighing 20–24 g) were anesthetized with a mixture of intraperitoneal xylazine (5 mg/kg) and ketamine (100 mg/kg). Transverse aortic constriction (TAC) was performed to induce cardiac hypertrophy and heart failure, as described previously (*9*, *10*).

Mice were divided into 4 groups, which were the sham ($n$=12), sham+atorvastatin ($n$=9), TAC ($n$=13), and TAC+atorvastatin ($n$=12) groups. Atorvastatin calcium (an HMG-CoA reductase inhibitor kindly provided by Pfizer Pharmaceutical Co., Ltd., Tokyo, Japan) was administrated at a daily dose of 5 mg/kg (dissolved in 10% ethanol and orally administrated by gavage) from day 2 after TAC. The dose of atorvastatin was determined according to a previous report (*11*). After echocardiography and left ventricular (LV) hemodynamic studies were done at 4 weeks following TAC, the mice were sacrificed and their hearts and lungs were extracted for further analysis. For histological examination, hearts were fixed in 10% formalin and stained with hematoxylin/eosin or Azan/Mallory, whereas the hearts used for Western blot analysis were snap-frozen in liquid nitrogen and stored at −80°C until use. Hearts for RNA analysis were stored in RNAlater liquid.

### Echocardiography

Transthoracic echocardiography was performed with a Sonos 4500 and a 15-6L MHz transducer (Philips, Eindhoven, the Netherlands). Mice were fixed in position without anesthesia. Two-dimensional short-axis views of the left ventricle were obtained for guided M-mode measurement of the posterior wall thickness (LVPWd), end-diastolic dimension (LVEDd), and end-systolic dimension (LVESd). LV fractional shortening (FS) and the ejection fraction (EF) were calculated as follows:

$$\text{LVFS} = (\text{LVEDd} - \text{LVESd})/\text{LVEDd} \times 100,$$

$$\text{LVEF} = [(\text{LV end-diastolic volume} - \text{LV systolic volume})/\text{LV end-diastolic volume}] \times 100.$$

The LV volume was calculated by the formula of Teichholz:

$$V = [7/(2.4 + D)] \times D^3,$$

where $V$ is the LV volume and $D$ is the LV dimension (*12*).

### Invasive Hemodynamic Study

LV hemodynamics were evaluated at 4 weeks after TAC. Mice from each group were anesthetized (lightly for TAC mice) and were ventilated as mentioned above. A Millar catheter was inserted *via* the right carotid artery and carefully introduced into the left ventricle to measure the systolic pressure (LVSP) and end-diastolic pressure (LVEDP). Maximum and minimum rates of LV pressure change (max $dP/dt$ and min $dP/dt$, respectively) as well as the contractility index (max $dP/dt$ divided by the pressure at the time of max $dP/dt$)

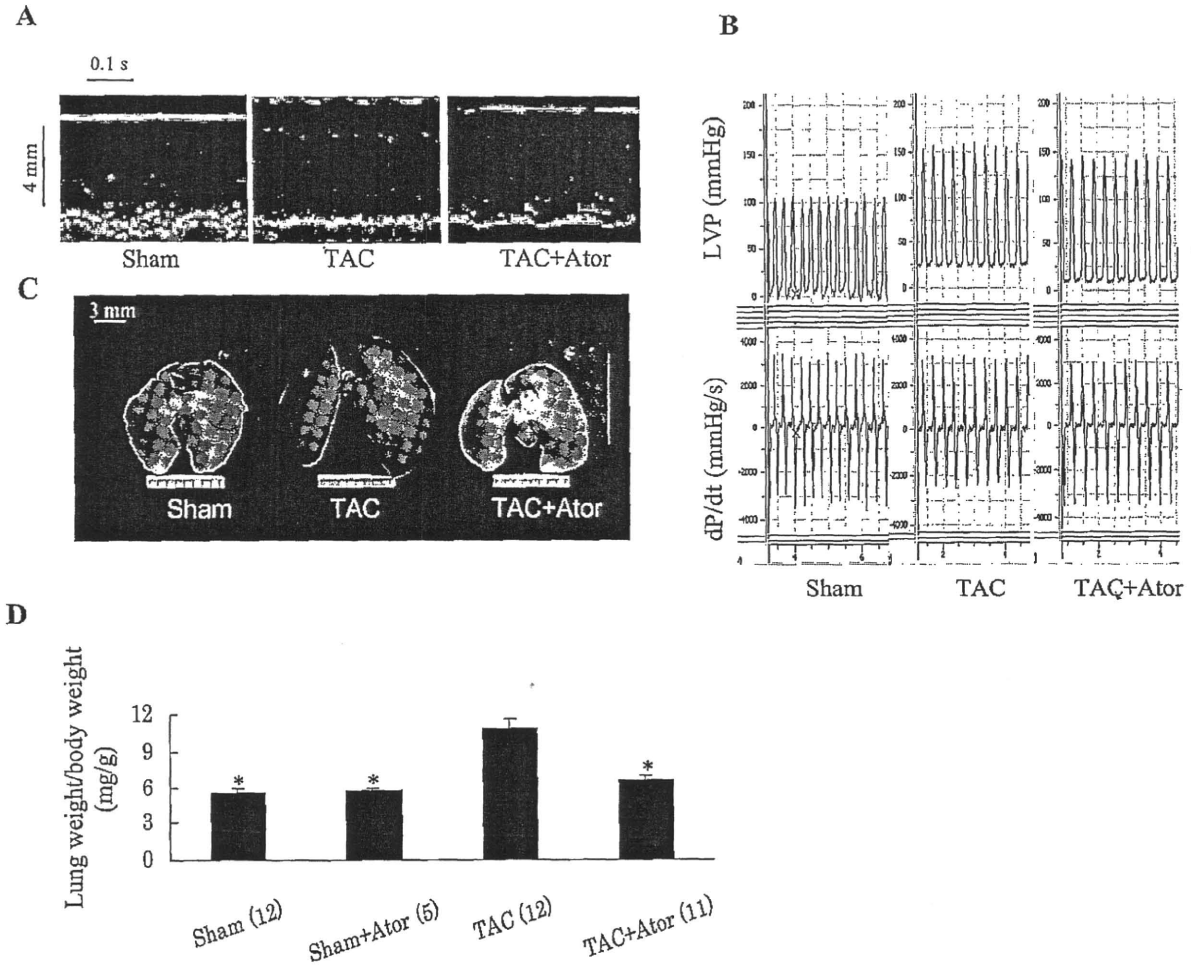


**Fig. 2.** *Improvement of cardiac function by atorvastatin (Ator). A: Representative M-mode echocardiographic images. B: Representative graph of left ventricular pressure and its rate of change (dP/dt), a lower end-diastolic pressure and higher min dP/dt were seen in the atorvastatin-treated mouse. C: Pulmonary congestion was ameliorated by atorvastatin at 4 weeks after TAC. D: The lung weight/body weight ratio (LW/BW) was significantly lower in atorvastatin-treated mice than in untreated TAC mice. ANOVA $p<0.0001$; *$p<0.01$ vs. TAC. The number of mice is shown in the parentheses.*

and the exponential time constant of relaxation ($\tau$) were calculated using a software program (Blood Pressure Module).

## Cell Culture

Ventricular myocytes were isolated from neonatal rats at 2 to 3 days of life and cultured as described previously (*8*). In brief, the cardiomyocytes were incubated for 72 h in Dulbecco's modified Eagle's medium supplemented with 10% fetal calf serum and then grown for 48 h under serum-free conditions. Subsequently, the cells were exposed to phenylephrine (PE, $10^{-4}$ mol/L) for 24 h in the presence or absence of atorvastatin ($10^{-7}$ to $10^{-5}$ mol/L). Cellular protein synthesis was evaluated on the basis of [$^3$H]leucine incorporation and EGFR activation was examined by immunoprecipitation Western blotting. To examine the effect of atorvastatin or the EGFR inhibitor AG1478 on ERK activation induced by PE, myocytes were exposed to PE $10^{-4}$ mol/L for 5 min with or without pretreatment for 30 min by atorvastatin $10^{-5}$ mol/L or AG1478 $10^{-6}$ mol/L.

## EGFR Phosphorylation

Cultured cardiomyocytes were exposed to $10^{-4}$ mol/L PE for 5 min with or without pretreatment for 30 min by atorvastatin ($10^{-5}$ or $10^{-7}$ mol/L). Then the cells were lysed by incubation for 20 min at 4°C in a buffer (50 mmol/L Tris-HCl, pH 7.3; 150 mmol/L NaCl; 2 mmol/L EDTA; 0.5% sodium fluoride; 10 mmol/L sodium pyrophosphate; 0.5 mmol/L $Na_3VO_4$; 100 μg/mL phenylmethylsulfonyl fluoride; 2 μg/mL aprotinin;

**Table 2. Left Ventricular Hemodynamics at 4 Weeks after TAC or Sham Operation**

| Group | LVSP (mmHg) | LVEDP (mmHg) | Max d*P*/d*t* (mmHg/s) | Min d*P*/d*t* (mmHg/s) | Contractility index | $\tau$ (ms) |
|---|---|---|---|---|---|---|
| Sham | 86±2.6*,† | 8.3±1.6*,† | 3,074±344 | 2,695±270‡ | 77.3±5.5* | 19.2±1.3# |
| Sham+Ator | 87±5.1*,† | 5.8±2.3*,† | 3,129±194 | 2,789±109 | 79.6±7.5# | 17.0±0.5* |
| TAC | 156±3.2 | 26.0±1.8 | 3,181±124 | 3,051±180 | 45.2±2.5 | 23.9±1.3 |
| TAC+Ator | 163±9.5 | 16.6±1.8* | 3,419±256 | 3,671±251 | 66.0±9.1# | 18.6±0.4* |
| ANOVA *p* | <0.0001 | <0.0001 | 0.7800 | 0.0033 | 0.0236 | 0.0010 |

TAC, transverse aortic constriction; Ator, atorvastatin, 5 mg/kg/day; LVSP, maximum left ventricular systolic pressure; LVEDP, left ventricular end-diastolic pressure; Max d*P*/d*t*, the steepest slope during the upstroke of the pressure curve; Min d*P*/d*t*, the steepest slope during the downstroke of the pressure curve; Contractility index, max d*P*/d*t* divided by the pressure at the time of max d*P*/d*t*; $\tau$, the exponential time constant of relaxation. *$p<0.01$, #$p<0.05$ *vs.* TAC, †$p<0.01$, ‡$p<0.05$ *vs.* TAC+Ator. The number of mice is 10 in each group except for Sham+Ator group ($n=5$). Data are mean±SEM.

protease inhibitor cocktail; and 1% Nonidet P-40). Immunoprecipitation of about 300 μg protein with Protein G Sepharose 4 Fast Flow (GE Healthcare, Uppsala, Sweden) and an antibody directed against the EGFR (Santa Cruz Biotechnology, Santa Cruz, USA; 1:100), immunoblotting using anti-PY20 to detect phosphorylation (BD Biosciences, San Jose, USA; 1:2,500) and anti-EGFR (Upstate Biotechnology, Lake Placid, USA; 1:500) to determine the EGFR expression were performed as described elsewhere (*8*).

*In vivo* EGFR phosphorylation was examined according to a previously described method (*13*) with some modifications. Briefly, mice were anesthetized with pentobarbital sodium (50 mg/kg). Phosphate buffer solution (10 mL) was perfused into the LV chamber of living hearts and then the heart was extracted and homogenized promptly in lysis buffer on ice. After centrifugation at 15,000 rpm for 10 min, the protein content in the supernatant was quantified and about 8,000 μg protein for each mouse was immunoprecipitated with Protein G Sepharose 4 Fast Flow and anti-EGFR (Santa Cruz Biotechnology; 1:100), and immunoblotting using anti-PY20 (BD Bioscience, 1:1,000) and anti-EGFR (Upstate, 1:500) were performed.

## Western Blot Analysis

Proteins were prepared from whole heart homogenates or cultured cardiomyocytes as described elsewhere (*14*). Immunoblotting was then performed using a mouse monoclonal antibody directed against ERK1/2 or anti–phospho-ERK1/2 antibodies (Santa Cruz Biotechnology). Immunoreactive bands were visualized by the enhanced chemiluminescence method (Amersham Biosciences, Buckinghamshire, UK) and then were quantified by densitometry with Scion Image software.

## Polymerase Chain Reaction

Total RNA was prepared from homogenized whole mouse hearts using RNA-Bee isolation reagent (Tel-Test Inc., Friendswood, USA) according to the manufacturer's protocol. The reverse transcription (RT)–polymerase chain reaction (PCR) was performed to generate cDNA from the extracted RNA. Expression quantitation of the genes for HB-EGF, MMP2, and MMP9 and brain natriuretic peptide (BNP) was determined using the TaqMan real-time PCR assay and an ABI PRISM7700 Sequence Detection System (Applied Biosystems, Foster City, USA), as described elsewhere (*9*). Oligonucleotide primers and TaqMan probes for mouse HB-EGF, MMP2, MMP9, BNP, and RNA 18S were all purchased from Applied Biosystems. Expression of a disintegrin and metalloproteinase (ADAM) 12 (primers: sense 5′-GACTCA TTGCCAATGGCTTCACGGA-3′, antisense 5′-ACTCAT GGAGCCTGGTGAATGGGTC-3′), and ADAM17 (primers: sense 5′-ACTGACAACTGCAAGGTGTGCT-3′, antisense 5′-TCCTGGATGGTGTCCATCCTCTGGT-3′) was detected by regular PCR.

## Measurement of Plasma Nitric Oxide

Blood was obtained from the right ventricle with a 25-gauge needle at the time of sacrificing the mice. The plasma concentrations of NOx ($NO_2$+$NO_3$) were measured with an autoanalyzer (ENO-10; Eicom Co., Kyoto, Japan), as described elsewhere (*15–17*). Samples were applied to an analytical column that was connected to a copperized cadmium reduction column to reduce $NO_2$ to $NO_3$, which was then reacted with Griess reagent, and the absorbance of the product was measured at 540 nm.

## Statistical Analysis

The unpaired Student's *t*-test was used for comparisons between two groups, while one-way ANOVA with post hoc analysis by the Tukey-Kramer or Fisher test was employed for multiple comparisons. Skewed data were log-transformed or log plus square root-transformed before testing was performed. Results were expressed as the means±SEM and values of $p<0.05$ were considered to indicate statistical significance.

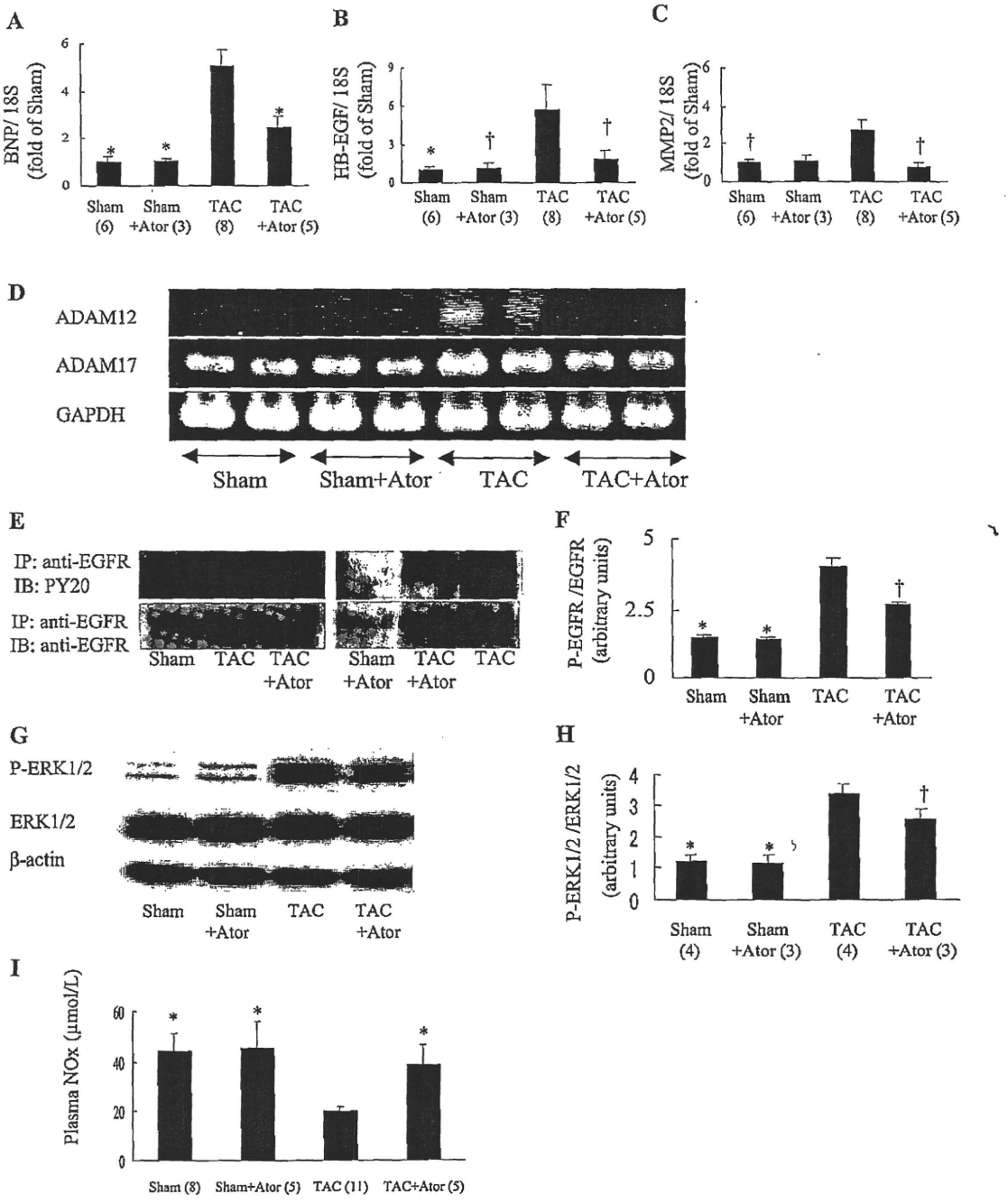


**Fig. 3.** *Atorvastatin (Ator) downregulated the expression of natriuretic peptide precursor type B (BNP), heparin-binding epidermal growth factor (HB-EGF), matrix metalloproteinases (MMPs), and EGFR and ERK1/2 activity in in vivo experiments. A–C: Expressions of the BNP, HB-EGF, and MMP2 genes were evaluated by TaqMan real-time quantitative PCR with 18S RNA as the internal control (ANOVA p values were <0.0001, 0.0012 and 0.0126, respectively). *p<0.01, †p<0.05 vs. TAC (statistical analysis for HB-EGF was performed after a log and square root transformation). The number of heart samples is shown in the parentheses. D: PCR results of ADAM12 and 17. E: Representative immunoblot of phospho-EGFR (P-EGFR) and EGFR. F: Ratio of P-EGFR to EGFR significantly increased in the hearts of TAC mice, while atorvastatin decreased it. G: Western blotting results of phospho-ERK1/2 (P-ERK1/2) and ERK1/2. H: Ratio of P-ERK1/2 to ERK1/2 markedly increased in the hearts of TAC mice, while atorvastatin decreased the ratio, β-actin served as the loading control (ANOVA p value <0.001). I: Plasma nitric oxide levels (ANOVA p value <0.0001). *p<0.01, †p<0.05 vs. TAC.*

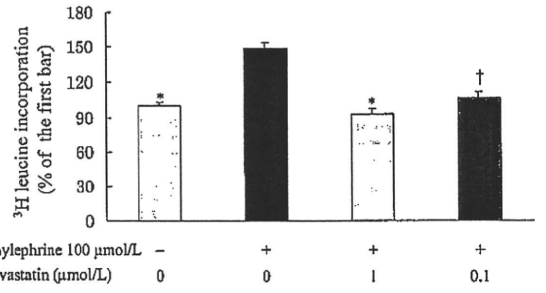


**Fig. 4.** *Atorvastatin inhibited protein synthesis of cultured neonatal rat cardiac myocytes. Phenylephrine enhanced protein synthesis and atorvastatin blocked this action. Each experiment was repeated at least 3 times. The first bar from the left side of the figure severed as the control. ANOVA $p<0.0001$; *$p<0.01$, †$p<0.05$ vs. phenylephrine alone.*

## Results

### Atorvastatin Ameliorates Cardiac Hypertrophy

Four weeks after TAC, the wet heart/body weight ratio (HW/BW) and cardiomyocyte cross-sectional surface area were increased in the TAC group compared with the sham group. No significant difference in heart weight was observed between the sham and sham+atorvastatin groups (Fig. 1F). Treatment with atorvastatin (TAC+atorvastatin group) ameliorated the hypertrophy of cardiomyocytes (Fig. 1A–C, F and G). We also observed an inhibitory effect of atorvastatin on myocardial and perivascular fibrosis (Fig. 1D, E, H and I). These findings indicate that atorvastatin therapy was able to inhibit cardiac hypertrophy and fibrosis in mice with LV pressure overload.

### Atorvastatin Slows the Onset of Heart Failure

Echocardiographic examination of conscious mice showed a significant increase of LVFS and LVEF, as well as a smaller LV chamber and thinner LV walls, in the TAC+atorvastatin group than in the TAC group (Table 1 and Fig. 2A), suggesting that atorvastatin both improved LV systolic function and inhibited LV remodeling.

We evaluated LV hemodynamics using a Millar pressure catheter before sacrificing the mice. LV pressure overload was similar in the TAC groups with and without atorvastatin treatment (Fig. 2B), but atorvastatin therapy increased the contractility index, in addition to decreasing LVEDP and $\tau$ (Table 2), indicating improvement of both systolic and diastolic function.

We have previously demonstrated that pulmonary edema is a reliable index of cardiac function in this model (*10*, *18*, *19*). Compared with that in sham mice, the lung/body weight ratio (LW/BW) was increased by 93% in TAC mice, whereas there was only a 17% increase of the LW/BW in the TAC+atorvastatin group (Fig. 2C, D).

No significant differences in the above-mentioned parameters were noted between the sham and sham+atorvastatin groups (Tables 1 and 2, Fig. 2D).

These findings strongly suggested that atorvastatin could slow the progression from hypertrophy to heart failure. We therefore investigated the mechanisms involved.

### Atorvastatin Downregulates Expression of MMPs and HB-EGF and BNP

Recent studies have revealed that the activation of MMP2 and MMP9 (*20*), or MMP3 (*21*), or ADAM12 (*8*) and ADAM17 (*22*, *23*) can induce the release of HB-EGF and subsequent EGFR transactivation, while upregulation of the expression of MMPs is reported to be associated with cardiac remodeling (*24*, *25*). In addition, statins are reported to effectively inhibit the activity of MMPs (*26*, *27*). Therefore, we examined cardiac expression of the genes for MMP2, MMP9, BNP, ADAM12 and 17 and HB-EGF in a TAC mouse model. As expected, compared with those in the sham group, the expressions of MMP2, BNP, and HB-EGF were increased by 3- to 5-fold in the TAC group, and atorvastatin markedly downregulated these genes (Fig. 3A–C). ADAM12 and 17 were also upregulated in TAC mice and inhibited by atorvastatin (Fig. 3D). There was no significant change in the MMP9 gene.

### Atorvastatin Inhibits Phosphorylation of EGFR and ERK1/2

Since ERK is recognized as one of the downstream elements of the EGFR signaling pathway and there are reports that statins can inhibit ERK activation (*28*), we examined the effect of atorvastatin on the activity of both EGFR and ERK1/2 in the hearts of mice. In the TAC group, myocardial EGFR and ERK1/2 activity was increased dramatically relative to that in the sham group, while atorvastatin markedly inhibited their activation (Fig. 3E–H).

### Atorvastatin Increases the Production of Nitric Oxide

As shown in Fig. 3I, the plasma level of NOx was markedly decreased in TAC mice at 4 weeks, and was significantly increased in TAC mice treated with atorvastatin.

### Atorvastatin Inhibits PE-Induced Protein Synthesis and EGFR Phosphorylation of Cardiomyocytes

In experiments using cultured neonatal rat cardiomyocytes, we found that protein synthesis was enhanced by PE and was dose-dependently inhibited by co-treatment with

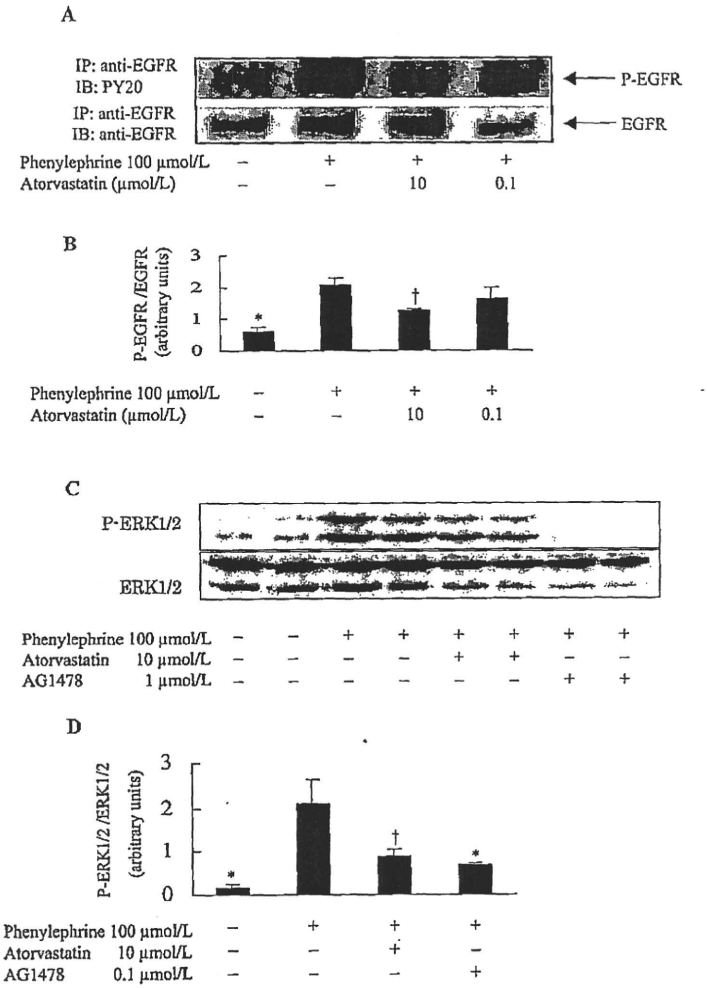


**Fig. 5.** *Atorvastatin inhibited the EGFR-ERK signaling pathway in vitro. EGFR phosphorylation induced by phenylephrine was significantly inhibited by atorvastatin (A and B). Atorvastatin or EGFR inhibitor AG1478 attenuated phenylephrine-stimulated ERK1/2 activation (C, D). After 30 min of exposure to atorvastatin or AG1478, phenylephrine was added and incubated for 5 min. Each experiment was repeated at least 3 times. ANOVA $p=0.001$, in both B and D; $^{*}p<0.01$, $^{\dagger}p<0.05$ vs. phenylephrine (Fisher test).*

atorvastatin (Fig. 4).

Based on our earlier report that EGFR activation by G-protein–coupled receptor (GPCR) agonists leads to the development of cardiac hypertrophy (*8*) and the findings that statins could inhibit the increase of cardiomyocyte protein synthesis stimulated by PE or angiotensin II (*29*), we hypothesized that atorvastatin may inhibit cardiomyocyte hypertrophy by preventing tyrosine phosphorylation of the EGFR. As a result, atorvastatin was found to inhibit EGFR phosphorylation induced by exposure to PE (Fig. 5A, B). In addition, PE induced the activation of ERK1/2, and atorvastatin inhibited that activation (Fig. 5C, D). Furthermore, the EGFR inhibitor AG1478 effectively attenuated PE-induced ERK activity (Fig. 5C, D). These data indicate that atorvastatin targets the GPCR–EGFR–mitogen-activated protein kinases (MAPKs) signaling pathway.

## Discussion

This study demonstrated that atorvastatin could markedly ameliorate cardiac remodeling induced by LV pressure overload. The beneficial effects of atorvastatin observed in this study included a decrease of cardiomyocyte hypertrophy, as well as improvements of pulmonary congestion, cardiac fibrosis, left ventricular contractility (LVFS and LVEF), and left ventricular diastolic indices (LVEDP and $\tau$). We also found that downregulation of MMPs and HB-EGF gene expression along with a reduction of EGFR phosphorylation

and ERK activity, and increase of nitric oxide production were associated with the suppression of cardiomyocyte hypertrophy and improvement of heart failure by atorvastatin.

Our finding that atorvastatin can improve both systolic and diastolic dysfunction is in good agreement with several recent clinical observations (*2–5*). Considering that a relatively low proportion of patients with non-ischemic heart failure receive statin therapy and a relatively high proportion of CHF patients have diastolic dysfunction, use of statins to treat CHF should be increased.

It is known that EGFR transactivation plays an important role in cardiovascular remodeling (*8, 20, 30–32*). It has been reported that activation of ADAM12 (*8*) or ADAM17 (*22*) could induce the release of HB-EGF and subsequent EGFR phosphorylation, which may eventually lead to cardiomyocyte hypertrophy, while inhibition of ADAM12 or administration of an HB-EGF neutralizing antibody blocked GPCR agonist–stimulated myocyte hypertrophy (*8*). A study performed by Lucchesi *et al.* supported the existence of a signaling pathway for pressure-induced HB-EGF release and subsequent EGFR activation in murine mesenteric resistance arteries (*20*). Zhang *et al.* confirmed that a similar pathway is activated to promote smooth muscle cell growth (*32*). Interestingly, a recent study reported that GPCR modification could inhibit cardiac hypertrophy *via* reduction of EGFR transactivation (*33*). The present study showed that atorvastatin could substantially decrease cardiac remodeling, as indicated by a reduction of LV wall thickness and LV dimensions as well as improvement of myocyte hypertrophy and perivascular fibrosis, findings that are consistent with the results of a recent pilot clinical trial (*4*) and several previous experimental studies (*28, 29, 34*). However, no study has yet examined whether or not statins can inhibit EGFR transactivation. In this study, we obtained evidence that atorvastatin could inhibit EGFR phosphorylation induced by pressure overload or the GPCR agonist PE. Since HB-EGF released from the cell membrane is soluble and the protein expression level is very low, it is not easy to detect by Western blot analysis. Instead, we found that myocardial expression of ADAM12 and 17 and HB-EGF was significantly increased in the presence of cardiac hypertrophy and heart failure, and that atorvastatin dramatically reversed the upregulation of these gene expressions, supporting the possibility that atorvastatin inhibits the MMPs–HB-EGF–EGFR signal pathway. We further confirmed that atorvastatin inhibited PE-induced ERK activation, while inhibition of EGFR by AG1478 dramatically attenuated PE-induced ERK activity, suggesting that ERK is located downstream of the EGFR activation pathway. Our *in vivo* data also showed that atorvastatin suppressed the increase of ERK activity in hypertrophied and failing hearts, which is in agreement with the results of previous studies (*28, 35*). Notably, this study provided the first direct evidence that *in vivo* phosphorylation increased in hypertrophic and failing hearts.

It should be noted that other actions of atorvastatin might have contributed to its inhibitory effect on cardiac remodeling in this study, including an antioxidant effect (*29, 36*), enhancement of nitric oxide availability (*37*), an antiinflammatory effect (*38*), and inhibition of neurohormonal activation (*39*).

In summary, atorvastatin effectively suppressed cardiac remodeling induced by pressure overload in mice, and inhibition of the activation of EGFR and ERK and increase in the nitric oxide production were possible mechanisms involved.

## References


1. Yan AT, Yan RT, Liu PP: Narrative review: pharmacotherapy for chronic heart failure: evidence from recent clinical trials. *Ann Intern Med* 2005; **142**: 132–145.
2. Fukuta H, Sane DC, Brucks S, Little WC: Statin therapy may be associated with lower mortality in patients with diastolic heart failure: a preliminary report. *Circulation* 2005; **112**: 357–363.
3. Horwich TB, MacLellan WR, Fonarow GC: Statin therapy is associated with improved survival in ischemic and nonischemic heart failure. *J Am Coll Cardiol* 2004; **43**: 642–648.
4. Sola S, Mir MQ, Lerakis S, Tandon N, Khan BV: Atorvastatin improves left ventricular systolic function and serum markers of inflammation in nonischemic heart failure. *J Am Coll Cardiol* 2006; **47**: 332–337.
5. Node K, Fujita M, Kitakaze M, Hori M, Liao JK: Short-term statin therapy improves cardiac function and symptoms in patients with idiopathic dilated cardiomyopathy. *Circulation* 2003; **108**: 839–843.
6. Kjekshus J, Dunselman P, Blideskog M, *et al*: A statin in the treatment of heart failure? Controlled rosuvastatin multinational study in heart failure (CORONA): study design and baseline characteristics. *Eur J Heart Fail* 2005; **7**: 1059–1069.
7. Tavazzi L, Tognoni G, Franzosi MG, *et al*: Rationale and design of the GISSI heart failure trial: a large trial to assess the effects of *n*-3 polyunsaturated fatty acids and rosuvastatin in symptomatic congestive heart failure. *Eur J Heart Fail* 2004; **6**: 635–641.
8. Asakura M, Kitakaze M, Takashima S, *et al*: Cardiac hypertrophy is inhibited by antagonism of ADAM12 processing of HB-EGF: metalloproteinase inhibitors as a new therapy. *Nat Med* 2002; **8**: 35–40.
9. Liao Y, Asakura M, Takashima S, *et al*: Benidipine, a long-acting calcium channel blocker, inhibits cardiac remodeling in pressure-overloaded mice. *Cardiovasc Res* 2005; **65**: 879–888.
10. Liao Y, Ishikura F, Beppu S, *et al*: Echocardiographic assessment of LV hypertrophy and function in aortic-banded mice: necropsy validation. *Am J Physiol Heart Circ Physiol* 2002; **282**: H1703–H1708.
11. Youssef S, Stuve O, Patarroyo JC, *et al*: The HMG-CoA reductase inhibitor, atorvastatin, promotes a Th2 bias and reverses paralysis in central nervous system autoimmune disease. *Nature* 2002; **420**: 78–84.
12. Teichholz LE, Kreulen T, Herman MV, Gorlin R: Problems in echocardiographic volume determinations: echocardio-

graphic-angiographic correlations in the presence of absence of asynergy. *Am J Cardiol* 1976; **37**: 7–11.
13. Iwamoto R, Yamazaki S, Asakura M, *et al*: Heparin-binding EGF-like growth factor and ErbB signaling is essential for heart function. *Proc Natl Acad Sci U S A* 2003; **100**: 3221–3226.
14. Privratsky JR, Wold LE, Sowers JR, Quinn MT, Ren J: AT1 blockade prevents glucose-induced cardiac dysfunction in ventricular myocytes: role of the AT1 receptor and NADPH oxidase. *Hypertension* 2003; **42**: 206–212.
15. Asanuma H, Kitakaze M, Node K, *et al*: Benidipine, a long-acting Ca channel blocker, limits infarct size *via* bradykinin- and NO-dependent mechanisms in canine hearts. *Cardiovasc Drugs Ther* 2001; **15**: 225–231.
16. Kitakaze M, Node K, Minamino T, Asanuma H, Kuzuya T, Hori M: A Ca channel blocker, benidipine, increases coronary blood flow and attenuates the severity of myocardial ischemia *via* NO-dependent mechanisms in dogs. *J Am Coll Cardiol* 1999; **33**: 242–249.
17. Tatsumi T, Akashi K, Keira N, *et al*: Cytokine-induced nitric oxide inhibits mitochondrial energy production and induces myocardial dysfunction in endotoxin-treated rat hearts. *J Mol Cell Cardiol* 2004; **37**: 775–784.
18. Liao Y, Takashima S, Asano Y, *et al*: Activation of adenosine A1 receptor attenuates cardiac hypertrophy and prevents heart failure in murine left ventricular pressure-overload model. *Circ Res* 2003; **93**: 759–766.
19. Liao Y, Asakura M, Takashima S, *et al*: Celiprolol, a vasodilatory beta-blocker, inhibits pressure overload-induced cardiac hypertrophy and prevents the transition to heart failure *via* nitric oxide–dependent mechanisms in mice. *Circulation* 2004; **110**: 692–699.
20. Lucchesi PA, Sabri A, Belmadani S, Matrougui K: Involvement of metalloproteinases 2/9 in epidermal growth factor receptor transactivation in pressure-induced myogenic tone in mouse mesenteric resistance arteries. *Circulation* 2004; **110**: 3587–3593.
21. Suzuki M, Raab G, Moses MA, Fernandez CA, Klagsbrun M: Matrix metalloproteinase-3 releases active heparin-binding EGF-like growth factor by cleavage at a specific juxtamembrane site. *J Biol Chem* 1997; **272**: 31730–31737.
22. Hinkle CL, Sunnarborg SW, Loiselle D, *et al*: Selective roles for tumor necrosis factor alpha–converting enzyme/ADAM17 in the shedding of the epidermal growth factor receptor ligand family: the juxtamembrane stalk determines cleavage efficiency. *J Biol Chem* 2004; **279**: 24179–24188.
23. Ohtsu H, Dempsey PJ, Eguchi S: ADAMs as mediators of EGF receptor transactivation by G protein–coupled receptors. *Am J Physiol Cell Physiol* 2006; **291**: C1–C10.
24. Sakata Y, Yamamoto K, Mano T, *et al*: Activation of matrix metalloproteinases precedes left ventricular remodeling in hypertensive heart failure rats: its inhibition as a primary effect of angiotensin-converting enzyme inhibitor. *Circulation* 2004; **109**: 2143–2149.
25. Moshal KS, Tyagi N, Moss V, *et al*: Early induction of matrix metalloproteinase-9 transduces signaling in human heart end stage failure. *J Cell Mol Med* 2005; **9**: 704–713.
26. Nicholls SJ, Cutri B, Worthley SG, *et al*: Impact of short-term administration of high-density lipoproteins and atorvastatin on atherosclerosis in rabbits. *Arterioscler Thromb Vasc Biol* 2005; **25**: 2416–2421.
27. Fukumoto Y, Libby P, Rabkin E, *et al*: Statins alter smooth muscle cell accumulation and collagen content in established atheroma of watanabe heritable hyperlipidemic rabbits. *Circulation* 2001; **103**: 993–999.
28. Patel R, Nagueh SF, Tsybouleva N, *et al*: Simvastatin induces regression of cardiac hypertrophy and fibrosis and improves cardiac function in a transgenic rabbit model of human hypertrophic cardiomyopathy. *Circulation* 2001; **104**: 317–324.
29. Takemoto M, Node K, Nakagami H, *et al*: Statins as antioxidant therapy for preventing cardiac myocyte hypertrophy. *J Clin Invest* 2001; **108**: 1429–1437.
30. Thomas WG, Brandenburger Y, Autelitano DJ, Pham T, Qian H, Hannan RD: Adenoviral-directed expression of the type 1A angiotensin receptor promotes cardiomyocyte hypertrophy *via* transactivation of the epidermal growth factor receptor. *Circ Res* 2002; **90**: 135–142.
31. Kagiyama S, Eguchi S, Frank GD, Inagami T, Zhang YC, Phillips MI: Angiotensin II–induced cardiac hypertrophy and hypertension are attenuated by epidermal growth factor receptor antisense. *Circulation* 2002; **106**: 909–912.
32. Zhang H, Chalothorn D, Jackson LF, Lee DC, Faber JE: Transactivation of epidermal growth factor receptor mediates catecholamine-induced growth of vascular smooth muscle. *Circ Res* 2004; **95**: 989–997.
33. Zhai P, Galeotti J, Liu J, *et al*: An angiotensin II type 1 receptor mutant lacking epidermal growth factor receptor transactivation does not induce angiotensin II–mediated cardiac hypertrophy. *Circ Res* 2006; **99**: 528–536.
34. Nadruz W Jr, Lagosta VJ, Moreno H Jr, Coelho OR, Franchini KG: Simvastatin prevents load-induced protein tyrosine nitration in overloaded hearts. *Hypertension* 2004; **43**: 1060–1066.
35. Miura S, Matsuo Y, Saku K: Simvastatin suppresses coronary artery endothelial tube formation by disrupting Ras/Raf/ERK signaling. *Atherosclerosis* 2004; **175**: 235–243.
36. Morikawa-Futamatsu K, Adachi S, Maejima Y, *et al*: HMG-CoA reductase inhibitor fluvastatin prevents angiotensin II–induced cardiac hypertrophy *via* Rho kinase and inhibition of cyclin D1. *Life Sci* 2006; **79**: 1380–1390.
37. Landmesser U, Engberding N, Bahlmann FH, *et al*: Statin-induced improvement of endothelial progenitor cell mobilization, myocardial neovascularization, left ventricular function, and survival after experimental myocardial infarction requires endothelial nitric oxide synthase. *Circulation* 2004; **110**: 1933–1939.
38. Rosenson RS, Tangney CC, Casey LC: Inhibition of proinflammatory cytokine production by pravastatin. *Lancet* 1999; **353**: 983–984.
39. Pliquett RU, Cornish KG, Peuler JD, Zucker IH: Simvastatin normalizes autonomic neural control in experimental heart failure. *Circulation* 2003; **107**: 2493–2498.

Cardiovascular Research (2008) 79, 600–610
doi:10.1093/cvr/cvn128

# Overexpression of endoplasmic reticulum-resident chaperone attenuates cardiomyocyte death induced by proteasome inhibition

Hai Ying Fu[1], Tetsuo Minamino[2]*, Osamu Tsukamoto[2], Tamaki Sawada[2], Mitsutoshi Asai[2], Hisakazu Kato[2], Yoshihiro Asano[2], Masashi Fujita[2], Seiji Takashima[2], Masatsugu Hori[2], and Masafumi Kitakaze[1]

[1]*Department of Cardiovascular Medicine, National Cardiovascular Center, Suita, Osaka 565-8565, Japan; and* [2]*Department of Cardiovascular Medicine, Osaka University Graduate School of Medicine, 2-2 Yamadaoka, Suita, Osaka 565-0871, Japan*

Received 17 December 2007; revised 8 April 2008; accepted 13 May 2008; online publish-ahead-of-print 28 May 2008

Time for primary review: 28 days

**KEYWORDS**
ER stress;
CHOP;
GRP78;
Proteasome inhibition;
Cardiomyocyte

**Aims** Proteasome inhibitors are a novel class of anticancer agents that induce tumour cell death via endoplasmic reticulum (ER) stress. Since ER stress is involved in the development of heart failure, we investigated the role of ER-initiated cardiomyocyte death by proteasome inhibition.

**Methods and results** Rat neonatal cardiomyocytes were used in this study. Proteasome activity was assayed using proteasome peptidase substrates. Cell viability and apoptosis were measured by 3-(4,5-dimethylthiazol-2-yl)-2,5-diphenol tetrazolium bromide and flow cytometry, respectively. Western blot analysis, real-time polymerase chain reaction (PCR) and reverse transcriptional PCR were used to detect the expression of protein and messenger ribonucleic acid (RNA). The location of overexpressed glucose-regulated protein (GRP) 78 was observed by confocal fluorescence microscopy. Proteasome inhibition induced cardiomyocyte death and activated ER stress-induced transcriptional factor ATF6, but not XBP1 (X-box binding protein 1), without up-regulating ER chaperones. ER-initiated apoptosis signalling, including cytosine-cytosine-adenine-adenine-thymine enhancer-binding protein (C/EBP) homologous protein (CHOP), c-Jun-N-terminal kinase (JNK), and caspase-12, was activated by proteasome inhibition. Short interference RNA targeting CHOP, but not the blockage of caspase-12 or JNK pathway, attenuated cardiomyocyte death. Overexpression of GRP78 suppressed both CHOP expression and cardiomyocyte death by proteasome inhibition.

**Conclusion** These findings demonstrate that proteasome inhibition induces ER-initiated cardiomyocyte death via CHOP-dependent pathways without compensatory up-regulation of ER chaperones. Supplement and/or pharmacological induction of GRP78 can attenuate cardiac damage by proteasome inhibition.

## 1. Introduction

Endoplasmic reticulum (ER) is an organelle that participates in the folding of membrane and secretory proteins. The conditions or stresses that interfere with ER function are named ER stress.[1] There are two ER stress-induced transcriptional factors to up-regulate ER-resident chaperones that promote the folding of accumulated proteins in ER: activating transcription factor 6 (ATF6) and X-box binding protein 1 (XBP1). ATF6 is cleaved in response to ER stress and the cleaved ATF6 traffics to nuclei to induce the expression of ER-resident chaperone.[2] In addition, ER stress induces *XBP1* messenger ribonucleic acid (mRNA) splicing, producing a new spliced *XBP1* mRNA.[3] The spliced XBP1 protein and cleaved ATF6 cooperatively up-regulate the expression of ER-resident chaperones that reduce ER stress.[4] Another important pathway to cope with ER stress is the degradation of misfolded proteins by the ubiquitin-proteasome system.[5] It is therefore conceivable that treatment of cells with proteasome inhibitors causes accumulation of misfolded proteins and ER stress. When the overload of misfolded proteins is not resolved, cell apoptosis signals are initiated from ER. This effect is mediated by increased expression of the transcription factor cytosine-cytosine-adenine-adenine-thymine enhancer-binding protein (C/EBP) homologous protein (CHOP) and activation of caspase-12 and c-Jun-N-terminal kinase (JNK).[6–8]

Recently, the ubiquitin-proteasome system is reported to be involved in the growth and survival of cells and

* Corresponding author. Tel: +81 6 6879 3472; fax: +81 6 6879 3473.
*E-mail address:* minamino@medone.med.osaka-u.ac.jp

considered as an attractive therapeutic target.[9] Proteasome inhibitors are usually short peptides linked to a pharmacophore that reacts with the active site of proteasome.[10] Based on the pharmacophores, proteasome inhibitors can be divided into several groups: peptide aldehydes (e.g. MG132), peptide boronates (e.g. PS341), and peptide epoxyketones (e.g. epoxomicin).[11] Among these proteasome inhibitors, bortezomib (PS341) has been used as anticancer agent against haematological malignancy and solid tumours.[12] Recently, the treatment with bortezomib was reported to be associated with cardiac failure in patients with lung cancer and multiple myeloma.[13,14] Furthermore, we have found that the accumulation of ubiquitinated proteins in failing heart samples from humans demonstrated the impairment of proteasome function in failing hearts.[15] These findings led us to hypothesize that the proteasome inhibition could cause cardiomyocyte death via an ER-dependent pathway. To test this hypothesis, we checked the role of ER-initiated apoptotic signalling in cardiomyocyte death when proteasome activity was pharmacologically inhibited. Furthermore, we also investigated whether overexpression of ER-resident chaperone could rescue cardiac cell death by proteasome inhibition. In the present study, we used MG132 and epoxomicin, two typical proteasome inhibitors, to investigate the effect of proteasome inhibition on cardiomyocytes. We also used tunicamycin, an inhibitor of N-linked glycosylation, as an ER stress inducer without affecting proteasome activity.

## 2. Methods

### 2.1 Materials

MG132, epoxomicin, and tunicamycin were purchased from Sigma Chemical Co. (St Louis, MO, USA). The antibodies for CHOP, XBP1, ATF6, and actin were obtained from Santa Cruz Biotechnology (Santa Cruz, CA, USA). The antibodies for phospho-JNK and JNK were obtained from Cell Signaling Technology, Inc. (Danvers, MA, USA). The antibodies for caspase-12 and HP1α were obtained from Sigma Chemical Co., while those for Lys-Asp-Glu-Leu (KDEL) and glyceraldehyde-3-phosphate dehydrogenase (GAPDH) were obtained from Assay Designs, Inc. (Ann Arbor, MI, USA) and Millipore Co. (Billerica, MA, USA). Z-Ala-Thr-Ala-Asp (Z-ATAD) and SP600125 were purchased from BioVision Inc. (Mountain View, CA, USA) and Calbiochem (San Diego, CA, USA), respectively.

### 2.2 Preparation of neonatal rat cardiomyocytes

Primary cardiomyocyte cultures were prepared from neonatal rat hearts as described previously.[16] All procedures were in accordance with the guiding principles of Osaka University School of Medicine, Position of the American Heart Association on Research Animal Use, and the Guide for the Care and Use of Laboratory Animals published by the US National Institute of Health (NIH Publication No. 85-23, revised 1996).

### 2.3 Proteasome activity assay

Chymotrypsin-like activities of proteasome were assayed using the fluorogenic peptides Suc-Leu-Leu-Val-Tyr-7-amino-4-methylcoumarin (LLVY-AMC) (Biomol, Plymouth Meeting, PA, USA) according to the method reported previously.[15] Briefly, after the treatment with MG132 or epoxomicin for 30 min, cultured rat neonatal cardiomyocytes were harvested, lysed in proteasome buffer (10 mmol/L Tris–HCl, pH 7.5, 1 mmol/L ethylene diamine tetraacetic acid (EDTA), 2 mmol/L adenosine-5'-triphosphate, 20% glycerol, and 4 mmol/L dithiothreitol), and centrifuged at 13 000 g at 4°C for 10 min. Then the supernatant (20 μg of protein) was incubated with proteasome activity assay buffer (0.05 mol/L Tris–HCl, pH 8.0, 0.5 mmol/L EDTA, 40 μmol/L LLVY-AMC) for 1 h at 37°C. The reaction was stopped by adding 0.9 mL of cold water and placing the reaction mixture on ice for at least 10 min. Subsequently, the fluorescence of the solution was measured by Fluorescence Microplate Reader (Gemini XS; Molecular Devices, Sunnyvale, CA, USA) with excitation at 380 nm (Ex) and emission at 440 nm (Em). All readings were standardized relative to the fluorescence intensity of an equal volume of free 7-amino-4-methylcoumarin (Sigma) solution (40 μmol/L).

### 2.4 Caspase-12 activity assay

Caspase-12 activity was assayed using its substrate ATAD-7-amino-4-trifluoromethyl coumarin. Cell lysate aliquots were assayed by Fluorescence Microplate Reader (Gemini XS; Molecular Devices) with 400 nm excitation and 505 nm emission filter according to the manufacturer's protocol (BioVision).

### 2.5 3-(4,5-Dimethylthiazol-2-yl)-2,5-diphenol tetrazolium bromide assay

Cardiomyocytes were seeded at $3 \times 10^4$/well in 96-well plates. After MG132 administration at appropriate conditions, cell numbers were measured with a water-soluble tetrazolium reagent [WST-8; 2-(2-methoxy-4-nitrophenyl)-3-(4-nitrophenyl)-5-(2,4-disulfophenyl)-2H-tetrazolium, monosodium salt] (Dojindo Laboratories, Kumamoto, Japan) according to the manufacturer's instructions. Cell viability was expressed as a percentage of the control. The wavelengths used in this assay were 450 nm (sample) and 630 nm (reference).

### 2.6 Western blot analysis

Cardiomyocytes were lysed in the buffer (0.15 mmol/L, NaCl 0.05 mmol/L Tris–HCl, pH 7.2, 1% Triton X-100, 1% sodium deoxycholate, 0.1% SDS) containing a protease inhibitor cocktail (Nakarai Tesque, Kyoto, Japan). Electrophoresis, immunoblotting, and detection were done as described previously.[15]

### 2.7 Reverse transcriptional polymerase chain reaction

After rat cardiomyocytes were treated with the drugs for 6 h, *XBP1* mRNA splicing was assessed using reverse transcriptional polymerase chain reaction (PCR) method. The primers that spanned the splice site are designed as followed: forward, ACGAGAGAAAACTCATGG; reverse, ACAGGGTCCAACTTGTCC (*Figure 1D*). This pair of primers can detect both spliced and unspliced *XBP1* at the size of 290 and 264 bp, respectively. The primers for GAPDH are forward, CATCAACGACCCCTTCATTGACCTCAACTA;reverse,TCCACGATGCCAAAGTTGTCATGGATGACC. PCR products were resolved on a 2% agarose gel and viewed by UV illumination.

### 2.8 Real-time quantitative polymerase chain reaction

We obtained samples after the drug treatment and then they were prepared according to the Omniscript Reverse Transcription Handbook (QIAGEN Inc., Hilden, Germany). The rat primers and probes used for quantification of glucose-regulated protein (GRP) 78, GRP94, CHOP, and GAPDH were all designed according to the manufacturer's protocol (Applied Biosystems, Foster City, CA, USA. https://www.appliedbiosystems.com/). Real-time PCR was performed with an ABI PRISM 7000 Sequence Detection System

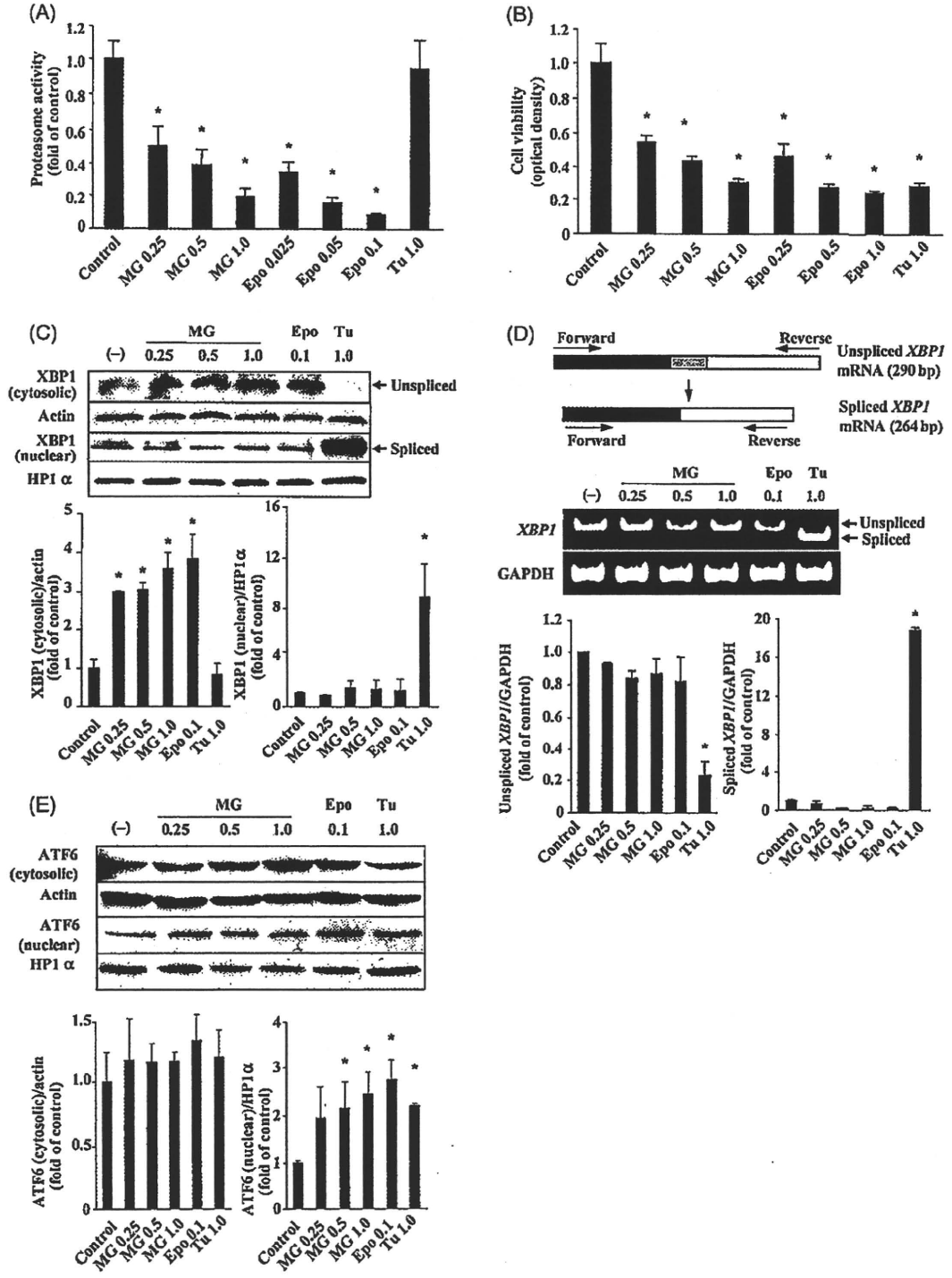


**Figure 1** . Effects of pharmacological proteasome inhibitors on the proteasome activity, cell death and endoplasmic reticulum stress-induced transcriptional factors in cultured cardiomyocytes. (*A*) Proteasome activity after the treatment with MG132 (MG) (0.25, 0.5, 1.0 μmol/L), epoxomicin (Epo) (0.025, 0.05, 0.1 μmol/L) or tunicamycin (Tu) (1.0 mg/mL) for 30 min. Experiments were repeated independently for three times ($n = 3$ in each experiment). (*B*) Cardiomyocyte viability after the treatment with MG, Epo or Tu for 48 h. Experiments were repeated independently for four times ($n = 6$ in each experiment). (*C*) Western blot analysis of spliced and unspliced X-box binding protein 1 (XBP1) proteins after the treatment with MG (0.25, 0.5, 1.0 μmol/L), Epo (0.1 μmol/L) or Tu (1.0 μg/mL) for 6 h. Actin and HP1α were used as the internal controls of cytosolic and nuclear fractions, respectively. (*D*) The upper panel shows the design of polymerase chain reaction (PCR) primers for *XBP1* messenger ribonucleic acid (mRNA) used in this study. This pair of primers can detect both unspliced and spliced *XBP1* mRNA. The middle and lower panels are representative and quantitative results of reverse transcriptional PCR for spliced and unspliced *XBP1* mRNA after the treatment with MG (0.25, 0.5, 1.0 μmol/L), Epo (0.1 μmol/L) or Tu (1.0 μg/mL) for 6 h. Glyceraldehyde-3-phosphate dehydrogenase was used as the internal control of mRNA expression. (*E*) Western blot analysis of ATF6 (activating transcription factor 6) in cytosolic and nuclear fractions after the treatment with MG (0.25, 0.5, 1.0 μmol/L), Epo (0.1 μmol/L) or Tu (1.0 μg/mL) for 6 h. The quantitative data in *C*, *D*, and *E* were achieved from three independent experiments. (Asterisk) $P < 0.05$ vs. control.

(Applied Biosystems) by the relative standard curve method. The thermal cycle reaction was performed as follows: 50°C for 2 min, 95°C for 10 min followed by 40 cycles at 95°C for 15 s, 60°C for 1 min. The target amount was determined from the relative standard curves constructed with serial dilutions of the control total cDNA.

## 2.9 Ribonucleic acid interference

We ordered four different short interfering ribonucleic acid (siRNA) from B-Bridge International, Inc. (Mountain View, CA, USA) to knock down CHOP mRNA (CHOP siRNA-1: 5′-CGAAGAGGAAGAAUCAAA-3′, siRNA-2: 5′-GGAAACAGCGACUGAAGGA-3′, siRNA-3: 5′-GGGACUGA GGGUAGACCAA-3′, siRNA-4: cocktail containing equal amounts of the above three types of siRNA). Rat cardiomyocytes were isolated and then incubated in Dulbecco's modified Eagle's medium (Invitrogen Co., Carlsbad, CA, USA). Opti-MEM (Invitrogen Co.), siRNA oligonucleotides (CHOP siRNA 1–4) (60 nmol/L) and Optifect (Invitrogen Co.) were added 4 h after cardiomyocyte isolation. As a negative control, cells were transfected with siRNA against firefly luciferase from Photinus pyralis (GL2 siRNA).

## 2.10 Flow cytometry

An Annexin V-fluorescein isothiocyanate (FITC) Apoptosis Detection Kit was purchased from Sigma. After the treatment of MG132, cardiomyocytes were washed twice with PBS and resuspended in binding buffer. FITC-Annexin V and propidium iodide were added according to the manufacturer's protocol. The mixture was incubated for 10 min in dark at room temperature and then cellular fluorescence was measured with a FACSscan flow cytometry (Becton, Dickinson and Company, Franklin Lakes, NJ, USA).

## 2.11 Adenovirus transduction

Recombinant adenovirus harbouring GRP78 gene was constructed as described previously,[17] and adenovirus harbouring LacZ was used as a control. Adenovirus was transfected 24 h after cardiomyocytes were isolated or 20 h after siRNA against CHOP was added. And the experiments were performed another 24 h after adenovirus infection.

## 2.12 Confocal fluorescence microscopy

Cardiomyocytes were observed by confocal microscopy (Radiance 2100 Laser Scanning System Bio-Rad, Hemei Hempstead, UK) and saved by LaserSharp 2000 (Bio-Rad). Alexa568 (red) (Invitrogen Co.) was scanned by helium/neon laser (wavelength 543 nm laser line) with long path 590 filter (560–700 nm excitation). Alexa488 (green) was captured by Argon laser (wavelength 488 nm laser line) with band path 500–550 IR filter (500–550 nm excitation). DAPI (blue) for nuclei staining of all cells was obtained in range of 400–470 nm excitation.

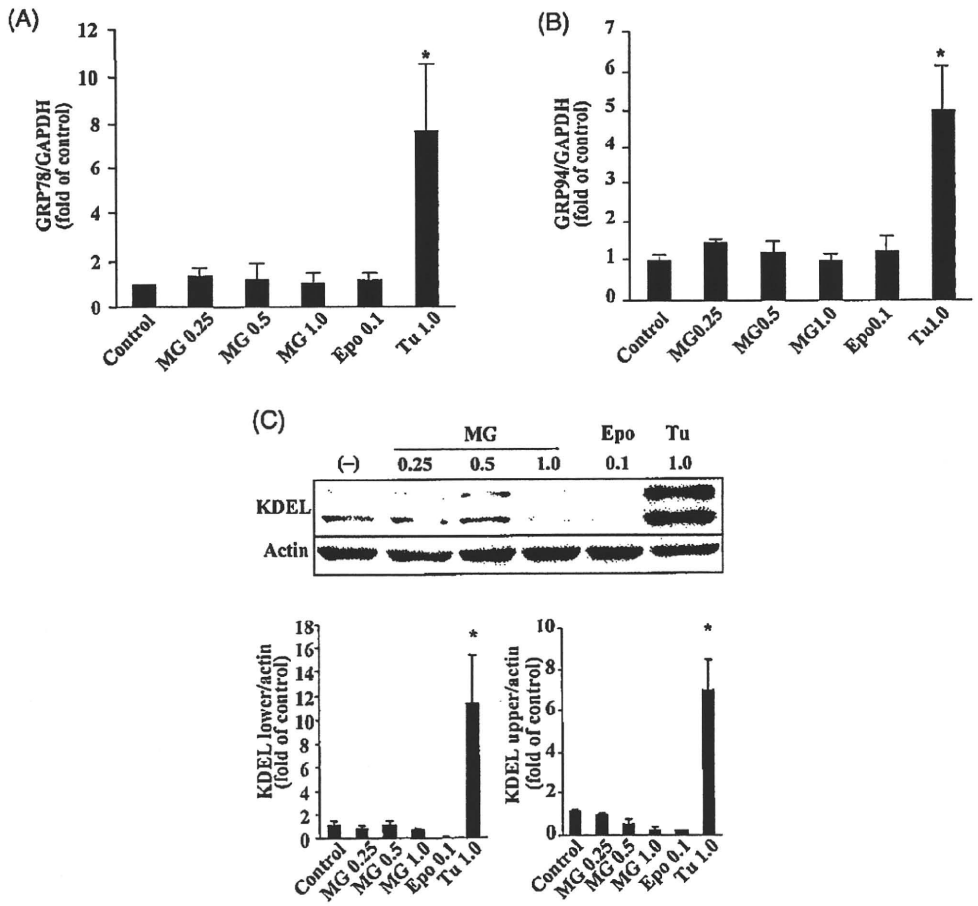


Figure 2 Endoplasmic reticulum chaperon expression by proteasome inhibition in cultured cardiomyocytes. Real-time polymerase chain reaction analysis of glucose-regulated protein (GRP) 78 (*A*) and GRP94 (*B*) ($n = 3$ in each experiment) and western blot analysis of Lys-Asp-Glu-Leu (KDEL) proteins (*C*) (upper and lower bands indicate GRP94 and GRP78, respectively) after the treatment with MG132 (MG) (0.25, 0.5, 1.0 μmol/L), epoxomicin (Epo) (0.1 μmol/L) or tunicamycin (Tu) (1.0 μg/mL) for 6 h. The western blot analysis and real-time PCR experiment were repeated for three times independently. (Asterisk) $P < 0.05$ vs. control.

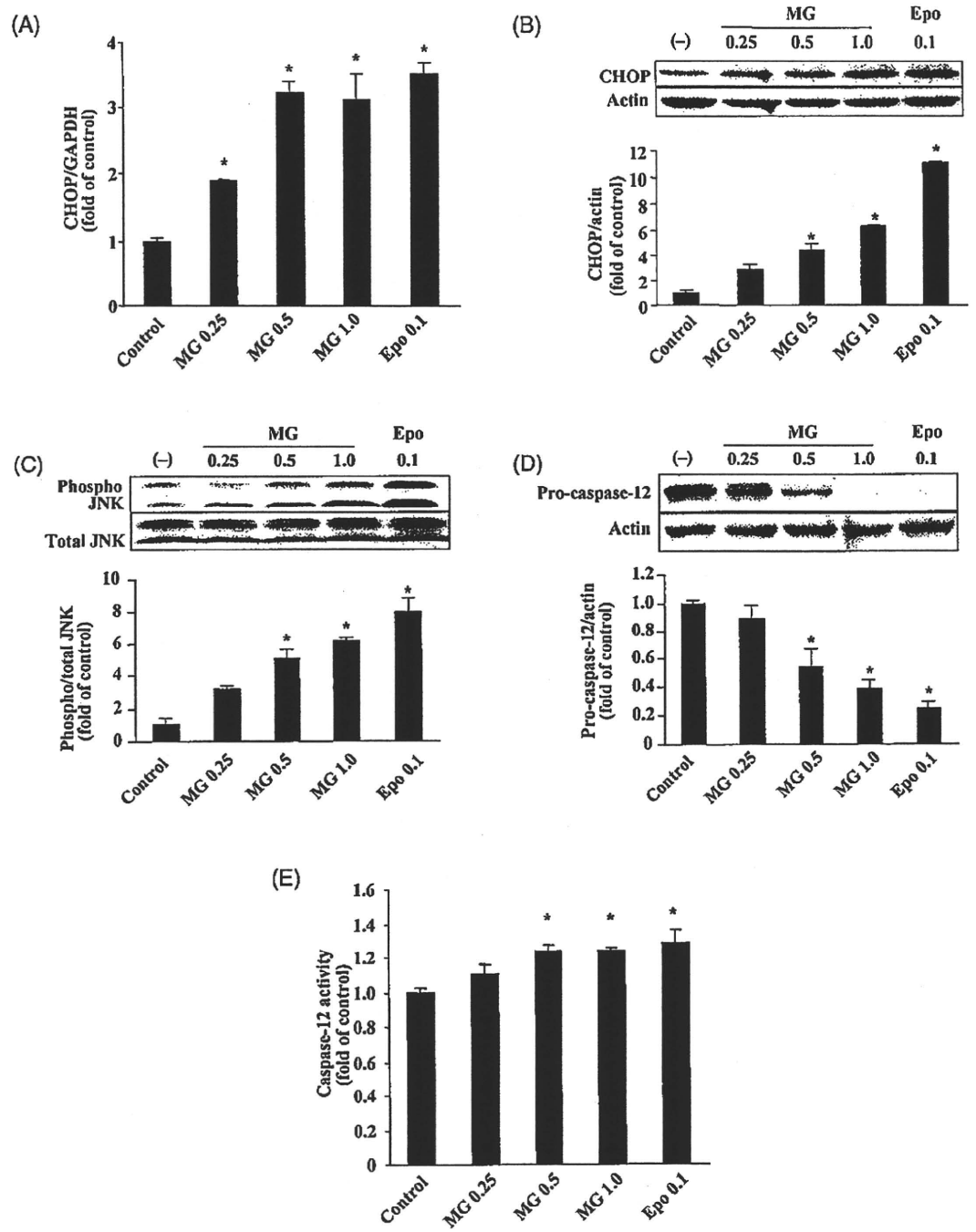


Figure 3 Activation of endoplasmic reticulum-initiated apoptosis signalling by proteasome inhibition in cultured cardiomyocytes. Real-time polymerase chain reaction (*A*) ($n = 3$ in each experiment) and western blot (*B*) analysis of CHOP [cytosine-cytosine-adenine-adenine-thymine (CCAAT) enhancer-binding protein (C/EBP) homologous protein] after the treatment with MG132 (MG) (0.25, 0.5, 1.0 μmol/L) or epoxomicin (Epo) (0.1 μmol/L) for 6 h. Western blot analysis of phospho-c-Jun-N-terminal kinase (JNK) (*C*) and pro-caspase-12 (*D*) after the treatment with MG (0.25, 0.5, 1.0 μmol/L) or Epo (0.1 μmol/L) for 1 and 6 h, respectively. (*E*) Caspase-12 activity after the treatment with MG (0.25, 0.5, 1.0 μmol/L) or Epo (0.1 μmol/L) for 6 h in cultured cardiomyocytes. Experiments were repeated independently for three times ($n = 3$ in each experiment). The quantitative data were achieved from three independent experiments. (Asterisk) $P < 0.05$ vs. control.

## 2.13 Statistical analysis

Data are expressed as the mean ± SEM. The results of cardiac proteasome activity, caspase-12 activity, cell viability and quantitative analysis of western blot analysis, real-time PCR, reverse transcription-PCR, and flow cytometry were compared by one-way factorial ANOVA followed by Bonferroni's correction. For all analyses, $P < 0.05$ was accepted as statistically significant.

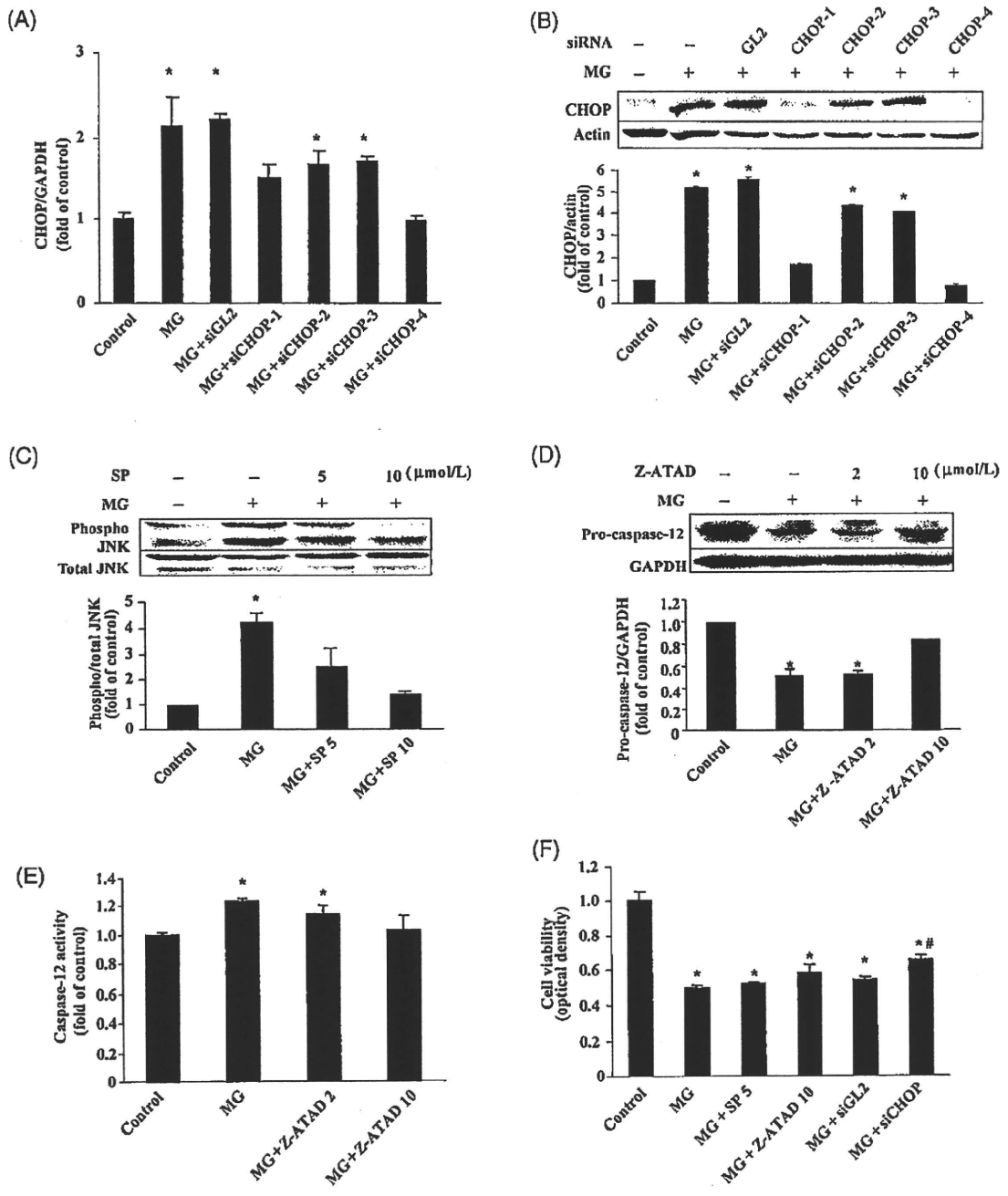


**Figure 4** Effects of blockade of endoplasmic reticulum (ER)-initiated apoptosis signalling on apoptosis by proteasome inhibition in cultured cardiomyocytes. Effects of four different types of siRNA (short interfering ribonucleic acid) targeting CHOP [CCAAT enhancer-binding protein (C/EBP) homologous protein] on *CHOP* mRNA (*A*) ($n = 3$ in each experiment) and protein expression (*B*) after the treatment with MG132 (MG) (1.0 μmol/L) for 6 h. (*C*) Effects of SP600125 on JNK (c-Jun-N-terminal kinase) phosphorylation after the treatment with MG (1.0 μmol/L) for 1 h. SP600125 was added 1 h before MG (1.0 μmol/L) administration. (*D*) and (*E*) Effects of Z-Ala-Thr-Ala-Asp (Z-ATAD) on caspase-12 activation after the treatment with MG (1.0 μmol/L) for 6 h. Z-ATAD was added 1 h before MG (1.0 μmol/L) administration ($n = 3$ in each experiment). (*F*) Results of cardiomyocyte viability by MTT [3-(4,5-dimethylthiazol-2-yl)-2,5-diphenol tetrazolium bromide] assay after the co-treatment with MG (1.0 μmol/L) and blockers of ER-initiated apoptosis signals ($n = 6$ in each experiment). Representative (*G*) and quantitative (*H*) data of cardiomyocyte apoptosis by flow cytometry ($n = 3$ in each experiment). The population of cells in the lower right quadrant of dot plot indicated apoptotic cardiomyocytes. Results of western blot and flow cytometry analysis represented three independent experiments, while the result of cell viability was from four independent experiments, respectively. (Asterisk) $P < 0.05$ vs. control; (Hash) $P < 0.05$ vs. MG (1.0 μmol/L).

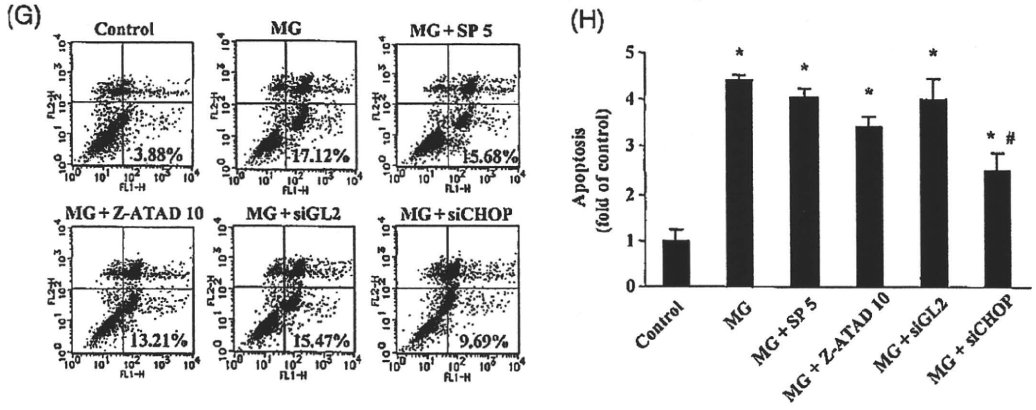


Figure 4 Continued.

## 3. Results

### 3.1 Proteasome activity and cell death by proteasome inhibition in cultured cardiomyocytes

Pharmacological proteasome inhibitors such as MG132 or epoxomicin dose-dependently decreased proteasome activity and reduced cell viability in rat-cultured cardiomyocytes. However, tunicamycin, an ER-stress inducer, induced cardiomyocyte death without inhibiting proteasome activity (*Figure 1A* and *B*).

### 3.2 Activation of endoplasmic reticulum stress-induced transcriptional factors and endoplasmic reticulum chaperone expression by proteasome inhibition in cultured cardiomyocytes

After the addition of MG132 or epoxomicin, protein level of unspliced XBP1 in cytosolic fraction, but not spliced XBP1 in nuclear fraction, was increased in rat-cultured cardiomyocytes (*Figure 1C*). The result of reverse transcriptional PCR demonstrated that either MG132 or epoxomicin did not change mRNA level of unspliced *XBP1* in cardiomyocytes (*Figure 1D*), suggesting that the increase in unspliced XBP1 protein level was due to the inhibition of its degradation by proteasome inhibition. In contrast, pharmacological ER stressor, tunicamycin, decreased unspliced *XBP1* mRNA expression and increased both mRNA and protein levels of spliced *XBP1* (*Figure 1C* and *D*). Proteasome inhibitors increased the protein level of ATF6 in the nuclear fraction in cultured cardiomyocytes (*Figure 1E*) to the similar extent as tunicamycin did. Importantly, proteasome inhibition did not induce the mRNA and protein expressions of either GRP78 or GRP94, although tunicamycin increased both of them (*Figure 2A–C*).

### 3.3 Activation of endoplasmic reticulum-initiated apoptosis signalling and cell death by proteasome inhibition in cultured cardiomyocytes

Proteasome inhibition by MG132 or epoxomicin increased both mRNA and protein levels of CHOP in rat-cultured cardiomyocytes (*Figure 3A* and *B*). In addition, it also induced JNK phosphorylation (*Figure 3C*) and caspase-12 activation (*Figure 3D* and *E*). CHOP siRNA 1 or 4, but not 2 or 3, significantly attenuated the MG132-induced increase in both mRNA and protein levels (*Figure 4A* and *B*). SP600125, an inhibitor of JNK phosphorylation, prevented the JNK phosphorylation by MG132 at both 5 and 10 μmol/L (*Figure 4C*). Z-ATAD, a caspase-12 inhibitor, attenuated the activation of caspase-12 by MG132 at 10, but not 2, μmol/L (*Figure 4D* and E). Cell viability analysed by 3-(4,5-dimethylthiazol-2-yl)-2,5-diphenol tetrazolium bromide (MTT) assay showed that siRNA targeting CHOP, but not SP600125 (5 μmol/L) or Z-ATAD (10 μmol/L) compound, prevented cell death induced by proteasome inhibition in rat-cultured cardiomyocytes (*Figure 4F*). Furthermore, consistent with the data of MTT assay, flow cytometry analysis showed that siRNA targeting CHOP, but not SP600125 or Z-ATAD, attenuated the apoptosis of cardiomyocyte induced by proteasome inhibition (*Figure 4G* and *H*).

### 3.4 Overexpression of glucose-regulated protein 78 attenuated endoplasmic reticulum stress and cell death by proteasome inhibition in cultured cardiomyocytes

Location of GRP78 overexpressed by adenovirus in cultured cardiomyocyte was almost consistent with that of protein disulphide isomerase, an ER-resident oxidoreductase (*Figure 5A*). The increase in GRP78 expression was confirmed by western blot analysis with the specific antibody of KDEL. Interestingly, GRP78 overexpression specifically inhibited the induction of CHOP, but not activation of caspase-12 or JNK (*Figure 5B–F*). Moreover, GRP78 overexpression dose-dependently decreased CHOP induction and increased cardiomyocyte viability (*Figure 5G–J*). Furthermore, the flow cytometry analysis also showed that overexpression of GRP78 attenuated apoptosis induced by proteasome inhibition in rat-cultured cardiomyocytes (*Figure 5K* and *L*). The overexpression of GRP78 combined with CHOP knockdown did not show additional effects on cardiomyocytes viability compared with GRP78 overexpression or CHOP knockdown alone (*Figure 5M*).

## 4. Discussion

The present study demonstrated that proteasome inhibitors, such as MG132 and epoxomicin, activated the ER stress-induced transcriptional factor ATF6, but not XBP1, without commeasurable expression of ER chaperone upon proteasome inhibition. Furthermore, proteasome inhibition induced cardiac apoptosis via CHOP-, but not JNK- or

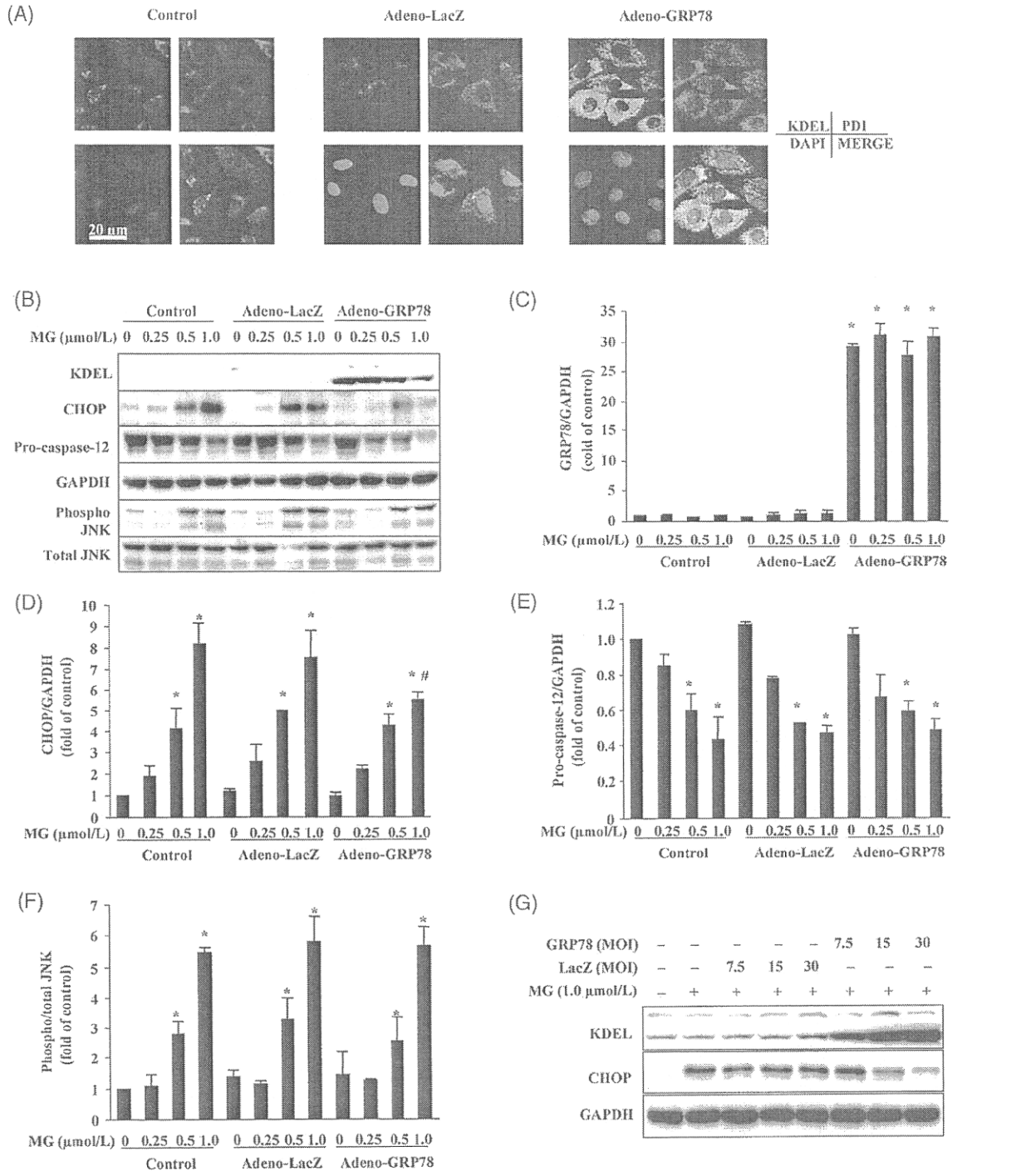


Figure 5 Overexpression of glucose-regulated protein (GRP) 78 reduced cardiomyocyte death by proteasome inhibition. (*A*) GRP78 was overexpressed by adenovirus at multiplicity of infection (MOI) 30 in cultured cardiomyocyte. Confocal fluorescence microscopy revealed that KDEL, PDI (protein disulphide isomerase) and DAPI were stained green, red and blue, respectively. (*B*) GRP78 expression, CCAAT enhancer-binding protein (C/EBP) homologous protein (CHOP) expression and activation of capase-12 were investigated after the treatment with MG132 (MG) (1.0 μmol/L) for 6 h at appropriate concentrations, while phospho-c-Jun-N-terminal kinase (JNK) was detected 1 h after MG administration. (*C-F*) Quantitative data of GRP78 expression (*C*), CHOP expression (*D*), casapase-12 activation (*E*) and JNK phosphorylation (*F*). (*G-I*) Representative (*G*) and quantitative (*H*, *I*) data for the expressions of endoplasmic reticulum chaperone (KDEL) and CHOP protein after GRP78 was overexpressed in a dose-dependent manner. MG (1.0 μmol/L) was administrated for 6 h. (*J-L*) Effects of overexpression of GRP78 on cardiomyocyte viability by 3-(4,5-dimethylthiazol-2-yl)-2,5-diphenol tetrazolium bromide (MTT) analysis (*J*) ($n = 6$ in each experiment) and cardiomyocytes apoptosis by flow cytometry (*K*, *L*) ($n = 3$ in each experiment) after MG (1.0 μmol/L) administration. (*M*) Effects of GRP78 overexpression combined with CHOP knockdown on cardiomyocyte viability by MTT analysis after proteasome inhibition ($n = 5$ in each group). Results of western blot and flow cytometry analysis represented three independent experiments, while the result of cell viability was from four independent experiments, respectively. (Asterisk) $P < 0.05$ vs. control; (Hash) $P < 0.05$ vs. MG (1.0 μmol/L).

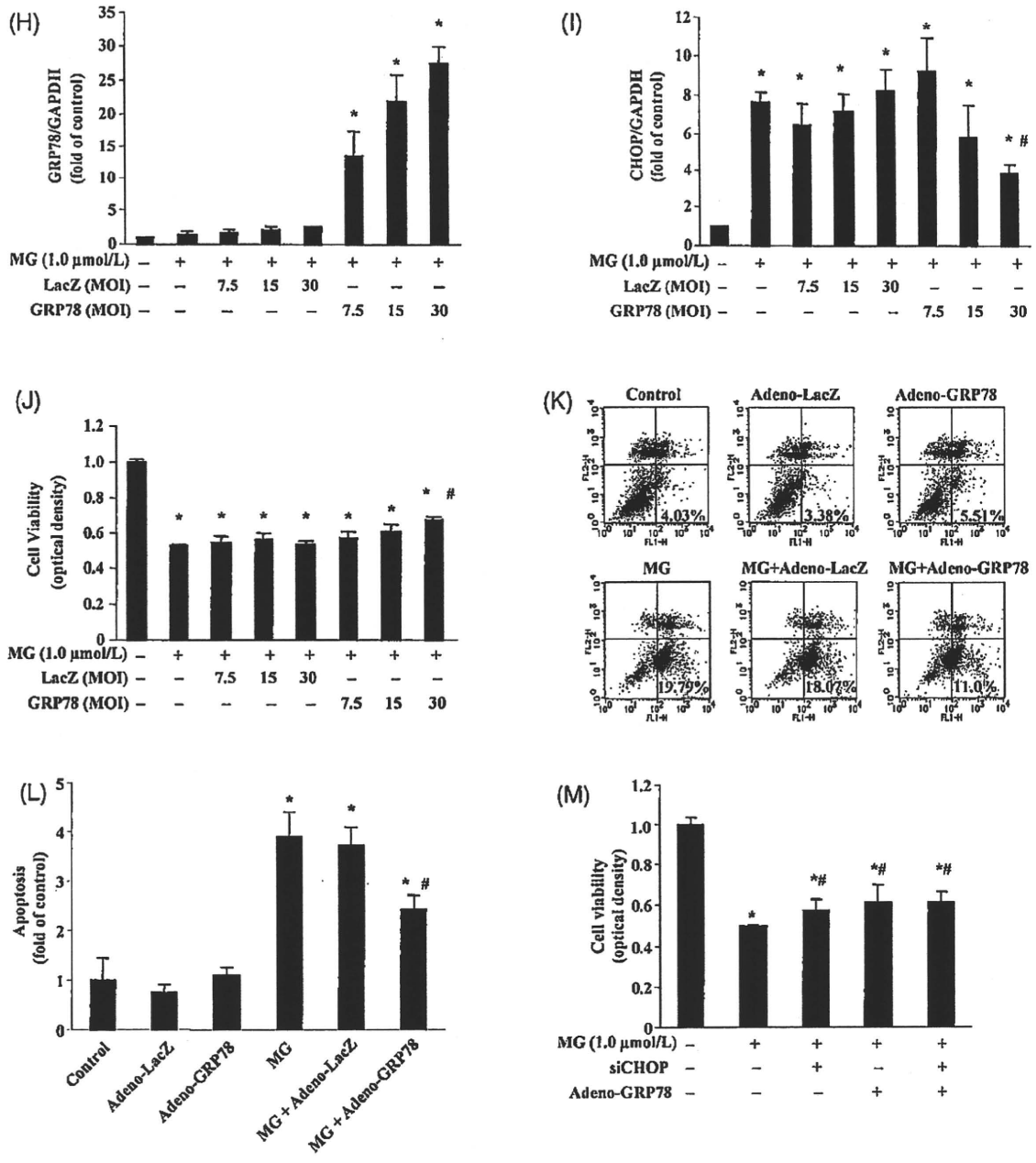


**Figure 5** Continued.

caspase-12-, dependent pathway. Adenovirus-mediated GRP78 overexpression attenuated CHOP expression and rescued cardiomyocyte death by proteasome inhibition. These results suggest that proteasome inhibition caused ER stress without a compensatory increase in ER chaperones and induced cardiac apoptosis via the CHOP-dependent pathway. Supplement and/or pharmacological induction of GRP78 may be a potential therapeutic tool to attenuate cardiac damage by proteasome inhibition.

After proteasome inhibition, cleaved ATF6 protein in the nuclear fraction was increased, which might be due to the decrease in ATF6 degradation by proteasome inhibition and/or increase in the ATF6 cleavage.[18] However, consistent with the previous report,[19] we could not detect the increase of spliced XBP1 at either mRNA or protein level, suggesting that XBP1 was not activated by proteasome inhibition. Since overexpression of cleaved ATF6 could up-regulate ER chaperone expression,[20,21] ER chaperone should be induced due to the increase in cleaved ATF6 by proteasome inhibition. In our study, however, ER chaperons were not up-regulated after proteasome inhibition, suggesting there are some mechanisms that may prevent up-regulation of ER chaperone by cleaved ATF6. Since unspliced XBP1 protein acts as a dominant negative inhibitor of the spliced form and deactivates ATF6 by heterodimerization,[19,22-24] one possible mechanism is that increased protein levels of unspliced XBP1 probably due to the decelerated degradation by proteasome inhibition